

Comenius University in Bratislava  
Faculty of Mathematics, Physics and Informatics

Analysis of Virtual Machine Based Obfuscators  
Master Thesis

Bratislava, 2023

Bc. Vladislav Hřčka

Comenius University in Bratislava  
Faculty of Mathematics, Physics and Informatics

Analysis of Virtual Machine Based Obfuscators  
Master Thesis

Study programme: Computer Science  
Field of study: Computer Science  
Department: Department of Computer Science  
Supervisor: RNDr. Jaroslav Janáček, PhD  
Consultant: Mgr. Peter Košíňár

Bratislava, 2023

Bc. Vladislav Hřčka



Comenius University Bratislava  
Faculty of Mathematics, Physics and Informatics

---

## THESIS ASSIGNMENT

**Name and Surname:** Bc. Vladislav Hrčka  
**Study programme:** Computer Science (Single degree study, master II. deg., full time form)  
**Field of Study:** Computer Science  
**Type of Thesis:** Diploma Thesis  
**Language of Thesis:** English  
**Secondary language:** Slovak  
**Title:** Analysis of Virtual Machine Based Obfuscators  
**Annotation:** The thesis describes a modern virtual machine based obfuscator and the general behavior of such machines. Known principles and tools for attacking this kind of protection are summarized. The thesis contains a proposal and an implementation of a solution that significantly facilitates analysis of code obfuscated with the modern virtual machine.  
**Aim:**

- describe virtual machine based obfuscators in general - summarize methods to deal with such kind of obfuscators
- analyze a specific virtual machine
- design and implement methods to devirtualize code protected with the specific machine

  
**Supervisor:** RNDr. Jaroslav Janáček, PhD.  
**Department:** FMFI.KI - Department of Computer Science  
**Head of department:** prof. RNDr. Martin Škoviera, PhD.  
**Assigned:** 14.12.2021  
**Approved:** 28.04.2023  
prof. RNDr. Rastislav Kráľovič, PhD.  
Guarantor of Study Programme

.....  
Student

.....  
Supervisor



Univerzita Komenského v Bratislave  
Fakulta matematiky, fyziky a informatiky

---

## ZADANIE ZÁVEREČNEJ PRÁCE

- Meno a priezvisko študenta:** Bc. Vladislav Hrčka  
**Študijný program:** informatika (Jednoodborové štúdium, magisterský II. st., denná forma)  
**Študijný odbor:** informatika  
**Typ záverečnej práce:** diplomová  
**Jazyk záverečnej práce:** anglický  
**Sekundárny jazyk:** slovenský  
**Názov:** Analysis of Virtual Machine Based Obfuscators  
*Analýza obfuskátorov založených na virtuálnych strojoch*  
**Anotácia:** Diplomová práca opisuje konkrétny moderný obfuskátor založený na virtuálnom stroji a vo všeobecnosti správanie takýchto virtuálnych strojov. Taktiež poskytuje prehľad známych princípov a nástrojov na prekonanie takejto formy ochrany programov. Diplomová práca obsahuje návrh a implementáciu riešenia, ktoré značne zjednodušuje analýzu kódu obfuskovaného daným moderným virtuálnym strojom.  
**Cieľ:**
  - popísať obfuskátory založené na virtuálnych strojoch vo všeobecnosti
  - zosumarizovať metódy na prekonanie tejto formy ochrany programov
  - analyzovať konkrétny virtuálny stroj
  - návrh a implementácia metód pre devirtualizovanie kódu chráneného daným virtuálnym strojom  
**Vedúci:** RNDr. Jaroslav Janáček, PhD.  
**Katedra:** FMFI.KI - Katedra informatiky  
**Vedúci katedry:** prof. RNDr. Martin Škoviera, PhD.  
**Dátum zadania:** 14.12.2021  
**Dátum schválenia:** 28.04.2023  
prof. RNDr. Rastislav Kráľovič, PhD.  
garant študijného programu

.....  
študent

.....  
vedúci práce

# Acknowledgements

Ďakujem hlavne kolegom z ESETu nielen za usmerňovanie a pomoc pri spisovaní práce, ale aj množstvo získaných skúseností a roky priateľskej atmosféry počas mojej práce vo firme. Osobitne chcem poďakovať svojmu konzultantovi Petrovi Košinárovi za hodnotné a príjemné odborné diskusie, koordinátorovi môjho vtedajšieho tímu Antonovi Cherepanovi za pridelenie tejto témy, a svojmu školiteľovi Jaroslavovi Janáčkovi za formálne zastrešenie a finálnu kontrolu práce.

# Abstrakt

Code Virtualizer je silný nástroj na obfuskáciu kódu Windows-ových aplikácií, ktorý slúži na ochranu citlivých častí kódu proti reverznému inžinierstvu pomocou použitia virtuálnych strojov. Okrem virtuálnych strojov, tento systém navyše zavádza niekoľko ďalších obfuskáčnych techník, ako napríklad vkladanie irelevantného kódu, kódovanie virtuálnych operandov, duplikácia virtuálnych opkódov, falošný tok riadenia, zlučovanie virtuálnych inštrukcií a ďalší vnorený virtuálny stroj. Virtuálne stroje Code Virtualizer sa stále častejšie používajú na škodlivé účely, ako napríklad na ochranu malvéru. V tejto práci analyzujeme súčasti virtuálneho stroja Code Virtualizer použitého vo vybranej vzorke malvéru a popisujeme náš poloautomatický prístup k prekonaniu jeho obfuskáčnych techník v primeranom čase. Demonštrujeme tento prístup na niekoľkých častiach bajtkódu obfuskovanej vzorky malvéru a porovnáваме výsledky s neobfuskovanou vzorkou na potvrdenie správnosti metódy. Náš prístup je založený na známej deobfuskačnej metóde, ktorá extrahuje sémantiku virtuálnych opkódov pomocou symbolického vykonávania s optimalizačnými pravidlami. Ďalej spracovávame časti bajtkódu a niektoré konštrukcie virtuálneho stroja ako konkrétne hodnoty namiesto symbolických, čo umožňuje spomínanej známej deobfuskačnej metóde automaticky prekonať aj ostatné obfuskáčne techniky. V práci postupne analyzujeme súčasti virtuálneho stroja, navrhujeme našu metódu deobfuskácie a popisujeme implementáciu tejto metódy.

# Abstract

Code Virtualizer is a powerful code obfuscation system for Windows applications that helps developers to protect sensitive code areas against Reverse Engineering with very strong obfuscation code, based on code virtualization. Apart from virtual machines, the obfuscation system additionally introduces several other obfuscation techniques such as insertion of junk code, encoding of virtual operands, duplication of virtual opcodes, opaque predicates, merging of virtual instructions, and another nested virtual machine. Code Virtualizer's virtual machines, with rest of the obfuscation techniques, have been increasingly being used for illicit purposes such as protection of malware. In this thesis we analyze the internals of a Code Virtualizer's virtual machine used in a malware sample and describe our semiautomatic approach to seeing through the obfuscation techniques in reasonable time. We demonstrate the approach on a few chunks of bytecode of the protected malware sample and compare the results against a non-obfuscated sample to confirm the validity of the method. Our approach is based on a known deobfuscation method that extracts the semantics of the virtual opcodes, using symbolic execution with simplifying rules. We further treat the bytecode chunks and certain internal constructs of the virtual machine as concrete values instead as symbolic ones, which enables the known deobfuscation method to deal with the additional obfuscation techniques automatically. In summary, we analyze the underlying parts of the virtual machine and gradually shape our deobfuscation approach. We describe our implementation of the approach at the end of the thesis.

# Contents

Introduction.....	1
1 Starting points.....	3
1.1 Documented techniques for deobfuscation of virtual machines .....	10
1.2 The Miasm framework .....	12
1.3 Choice of virtual machine .....	13
2 CV's virtual machine entry – vm_entry .....	15
3 Virtual machine initialization .....	18
4 Virtual instructions .....	21
4.1 Virtual instructions of the second virtual machine .....	25
4.2 The initial virtual instruction.....	32
4.3 Initially executed virtual instructions.....	38
5 Automating analysis of the first virtual machine .....	45
6 Description of our final VM analyzer code .....	52
7 Future work .....	55
Conclusion .....	56
References.....	57



# List of Figures

Figure 1. Illustration of bytecode, where all opcodes and operands are virtual.....	3
Figure 2. Illustration of the relationship between bytecode and the VM's interpreter.....	5
Figure 3. Illustration of Switch Dispatch (assembly jump table), where R0 is a virtual register .....	6
Figure 4. Illustration of Direct Threading .....	7
Figure 5. Overview of the virtualization process .....	9
Figure 6. Entry point to the virtual machine .....	15
Figure 7. A part of <code>vm_entry</code> of the virtual machine decompiled with Ghidra.....	16
Figure 8. Function used to unpack <code>NsPack</code> in ClamAV .....	16
Figure 9. A block of code in Miasm's symbolic execution (left) and a part of the same block in IDA's decompiler (right) .....	17
Figure 10. Miasm's symbolic execution of a <code>vm_pre_init()</code> showing parameters supplied to <code>vm_init()</code> .....	18
Figure 11. Busy-waiting for interpreter in <code>vm_init()</code> .....	19
Figure 12. <code>vm_init()</code> summary.....	20
Figure 13. Virtual instruction table .....	21
Figure 14. The first virtual instruction in the table .....	21
Figure 15. One of the <code>vm_pre_init()</code> functions .....	22
Figure 16. Miasm's symbolic execution of the first virtual instruction (function at <code>0x0FF2DB</code> ) .....	22
Figure 17. Miasm's symbolic execution of the first block of <code>vm2_init()</code> .....	23
Figure 18. Miasm's symbolic execution of the first block of <code>vm_init()</code> .....	24
Figure 19. A part of the second virtual instruction table.....	25
Figure 20. Virtual instructions in the structure of the virtual machines.....	26
Figure 21. The initial virtual instruction of the second VM.....	27
Figure 22. Bytecode of the virtual instruction.....	27
Figure 23. Destination address and memory modified by the second virtual instruction .....	27
Figure 24. Destination address and memory modified by the third virtual instruction.....	28
Figure 25. The conditional branch and delta of the stack pointer of the fourth virtual instruction.....	28
Figure 26. Destination address and memory modified by the fourth virtual instruction .....	29
Figure 27. Call graph generated from memory assignments and the VPC .....	31
Figure 28. Virtual instructions in the structure of the virtual machines.....	32
Figure 29. Control flow graph of the initial virtual instruction.....	33
Figure 30. Beginning of the prologue finishing context switch of the second VM .....	34
Figure 31. Virtual registers of the second machine being mapped back to the native ones at the end of the virtual instruction .....	35
Figure 32. Last few virtual instructions executed before mapping the virtual registers back to the native ones .....	37
Figure 33. Zeroing out an internal register.....	40
Figure 34. Storing the stack pointer in an internal register .....	42
Figure 35. Part of the fourth virtual instruction .....	43
Figure 36. Part of the fourth virtual instruction performing a pop-like operation .....	44
Figure 37. Part of the fourth virtual instruction performing a PUSH operation .....	44
Figure 38. The first processed bytecode block.....	46
Figure 39. Expressions that can be further simplified.....	47
Figure 40. Code of the processed bytecode.....	48

Figure 41. Data accessed by the code – <code>ServiceStatus</code> .....	48
Figure 42. Function whose pointer is used in the code .....	49
Figure 43. Destination address of the bytecode .....	49
Figure 44. Setting return address of the API call .....	50
Figure 45. Body of the code's loop .....	50
Figure 46. The same part of code in the non-obfuscated binary .....	51

# List of Tables

Table 1. Miasm's IR semantics.....	13
Table 2. Statistics of the initial virtual instruction .....	33
Table 3. Statistics of the first executed virtual instruction.....	41
Table 4. Statistics of the second executed virtual instruction .....	41
Table 5. Statistics of the third executed virtual instruction.....	43
Table 6. Statistics of the fourth executed virtual instruction.....	43
Table 7. Statistics of the first processed bytecode block.....	51

# Introduction

Reverse engineering is in terms of software-engineering process of analyzing functionality and behavior of certain software in order to get insight into its overall capabilities or achieve utter understanding of how its features are implemented and work. Initially, one often needs to partially recover the original source code out of an already compiled binary to perform reverse engineering – the source code cannot be usually completely recovered since some information is lost during the compilation process.

Techniques intended to hinder reverse engineering – make the source code difficult to read and understand – are called obfuscation techniques. Such techniques emerged as a way to address the need to protect intellectual property against infringements, such as counterfeiting and patent abuse in both software and hardware products. The protection aspect is a strong motivation for investing in research and development of the obfuscation techniques. The techniques are not meant to be bullet-proof, they are just supposed to discourage majority of the adversaries by forcing them to invest a substantial amount of time and means into overcoming the protection to recover the original source code.

Obfuscation techniques became later misused for illicit purposes such as protection of malware. Obfuscation often breaks patterns in the code and behavior of malware and that turns previous detection rules for non-obfuscated versions useless. Moreover, patterns in the obfuscated code can be different from sample to sample or contain significant overlaps with legitimate applications obfuscated using the same obfuscator – one cannot just consider all obfuscated code to be malicious.

This naturally resulted in an evolution of sort of counter-countermeasures – deobfuscation techniques that recover the original source code and revert the effects of the obfuscation techniques. They are primarily intended to facilitate analysis and detection of protected malware. The thesis deals with a specific type of protection – virtual-machine based obfuscation.

The first chapter is a comprehensive introduction into the field and thesis with several subchapters that describe general structure of virtual machine based obfuscators and compare them against the standard virtual machines; summarize known and unique techniques to deal with the obfuscation; introduce featured libraries and the virtual machine based obfuscator that

we are going to analyze in the further chapters. The remaining chapters progressively analyze underlying parts of the chosen obfuscator and shape the design of our deobfuscation method.

This thesis has been written in cooperation with ESET, published at blog WeLiveSecurity [1], and presented at few international cyber-security and reverse-engineering conferences: REcon (Montreal), CodeBlue (Tokyo), and SecTor (Toronto).

# 1 Starting points

This chapter initially summarizes known information about virtual machine based obfuscators and methods to recover the underlying original code. It afterwards introduces the analyzed virtual machine and tools used to design our deobfuscation method.

**General structure of virtual machines.** Virtual machines (VMs) can be divided into two main categories:

1. System virtual machines – support execution of complete operating systems (e.g., various VMWare products, VirtualBox)
2. Process virtual machines – execute individual programs in an OS-independent environment (e.g., Java, the .NET Common Language Runtime)

Here, we are interested only in the second category – process virtual machines – and we will briefly describe certain parts of their internal anatomy necessary to understand the rest of this paper.

Process virtual machines run as normal applications on their host OSes, and in turn run programs whose code is stored as OS-independent **bytecode** (Figure 1) that represents a series of instructions – an application – of a virtual ISA (instruction set architecture) [2].



*Figure 1. Illustration of bytecode, where all opcodes and operands are virtual*

One can also think about bytecode as a sort of **intermediate representation (IR)**; an abstract representation of code consisting of a specific instruction set that resembles assembly more than a high-level language. It is also known as intermediate language.

The use of IR is convenient in terms of code reusability – when one needs to add support for a new architecture or CPU instruction set, it is easier to convert it to the IR instead of writing all the required algorithms again. Another benefit is that it can simplify the application of some optimization algorithms.

One can generally translate both high- and low-level languages into an IR. Translation of a higher-level language is known as “lowering”, and similarly translation of a lower-level one, “lifting”.

The following example lifts an assembly block `bb0` into a block with the pseudo-IR code `irb0`. All assembly instructions are translated into a set of IR operations and individual operations in sets do not affect each other, where `ZF` stands for zero flag and `CF` for carry flag:

`bb0:`

```
MOV R8, 0x05
SUB AX, DX
XCHG ECX, EDX
```

`irb0:`

```
R8 = 0x05

EAX[:0x10] = EAX[:0x10] - EDX[:0x10]
ZF = EAX[:0x10] - EDX[:0x10] == 0x00
CF = EAX[:0x10] < EDX[:0x10]
...

ECX = EDX
EDX = ECX
```

Modern process VMs usually provide a compiler that can lower code written in a high-level language -- one that is easy to understand and comfortable to use – into the respective bytecode.

A VM’s **ISA** generally defines the supported instructions, data types and registers, among other things, that naturally must be implemented by a virtual ISA as well.

Instructions consist of the following parts:

- **opcodes** – operation codes that specify an instruction
- **operands** – parameters of the instructions

ISAs often use two well-known virtual registers:

- **virtual program counter** (VPC) – a pointer to the current position in the bytecode
- **virtual stack pointer** – a pointer to pre-allocated virtual stack space used internally by the VM

The virtual stack pointer does not have to be present in all VMs; it is common only in a certain type of VM – stack-based ones. [3]

We will refer to the instructions and their respective parts of a virtual ISA simply as **virtual instructions**, **virtual opcodes**, and **virtual operands**. We sometimes omit the explicit use of “virtual” when it is obvious that we are talking about the virtual representation.

An OS-dependent (Figure 2) executable file – **interpreter** – processes the supplied bytecode and sequentially interprets the underlying virtual instructions thus executing the virtualized program.

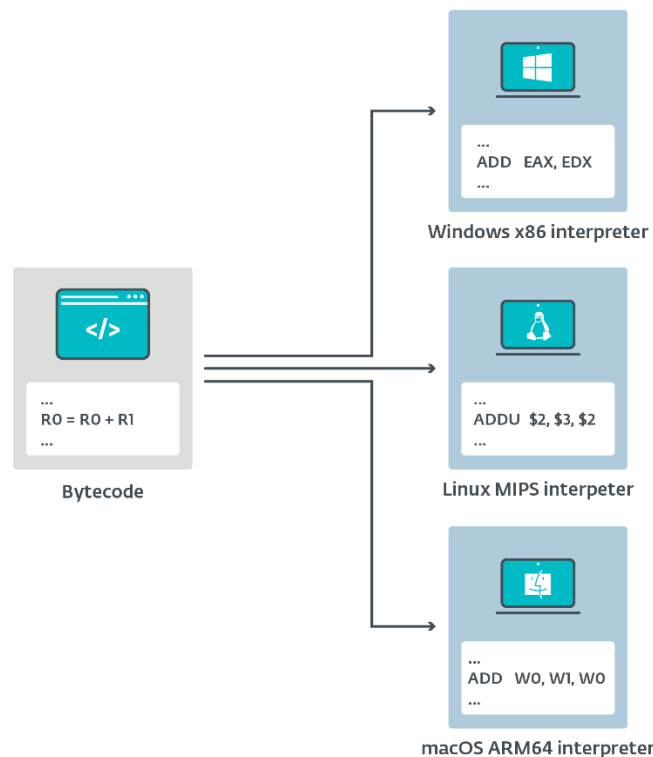


Figure 2. Illustration of the relationship between bytecode and the VM’s interpreter

Transfer of control from one virtual instruction to the next during interpretation needs to be performed by every VM. This process is generally known as **dispatching**. There are several documented dispatch techniques such as: [4]

- Switch Dispatch – the simplest dispatch mechanism where virtual instructions are defined as case clauses and a virtual opcode is used as the test expression (Figure 3)
- Direct Call Threading – virtual instructions are defined as functions and virtual opcodes contain addresses of these functions



- Direct Threading – virtual instructions are defined as functions again; however, in comparison to Direct Call Threading, addresses of the functions are stored in a table and virtual opcodes represent offsets to this table. Each function should indirectly call the following one according to the specification (Figure 4)

The body of a virtual opcode in the interpreter's code is usually called a **virtual handler** because it defines the behavior of the opcode and handles it when the virtual program counter points to a location in the bytecode that contains a virtual instruction with that opcode.

By **context**, regarding VMs, we mean a sort of virtual process context: each time a process is removed from access to the processor during process switching, sufficient information on its current operating state – its context – must be stored such that when it is again scheduled to run on the processor, it can resume its operation from an identical position. [5]

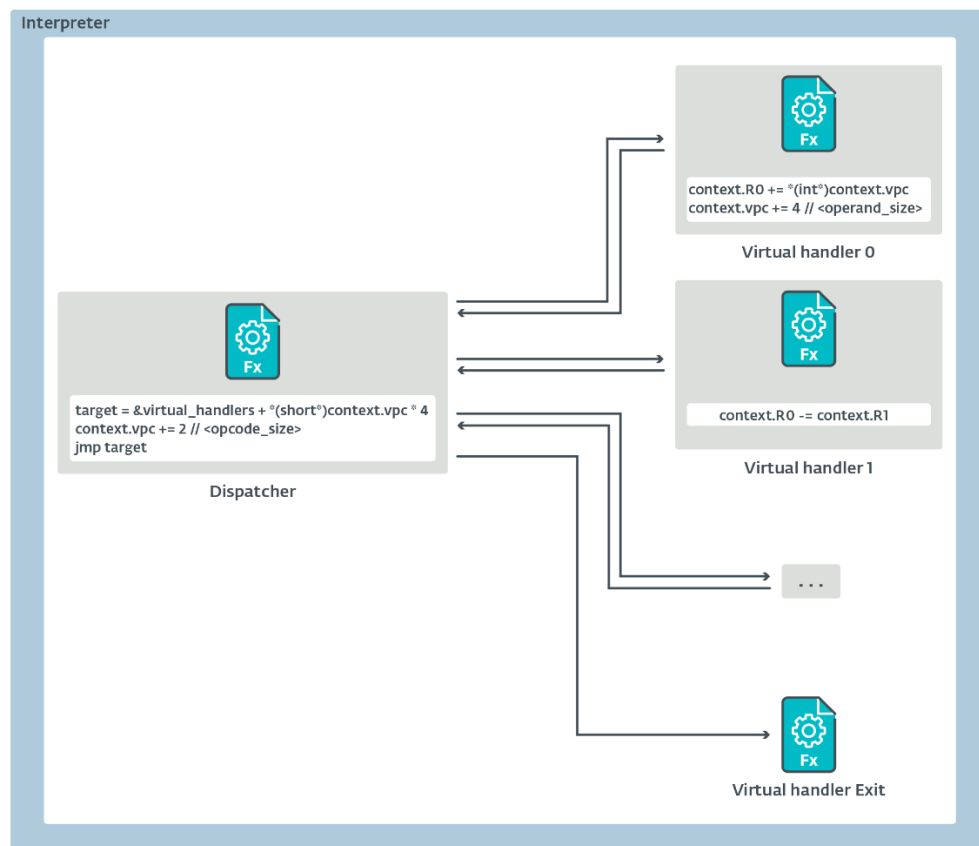


Figure 3. Illustration of Switch Dispatch (jump table in assembly), where  $R0$  is a virtual register

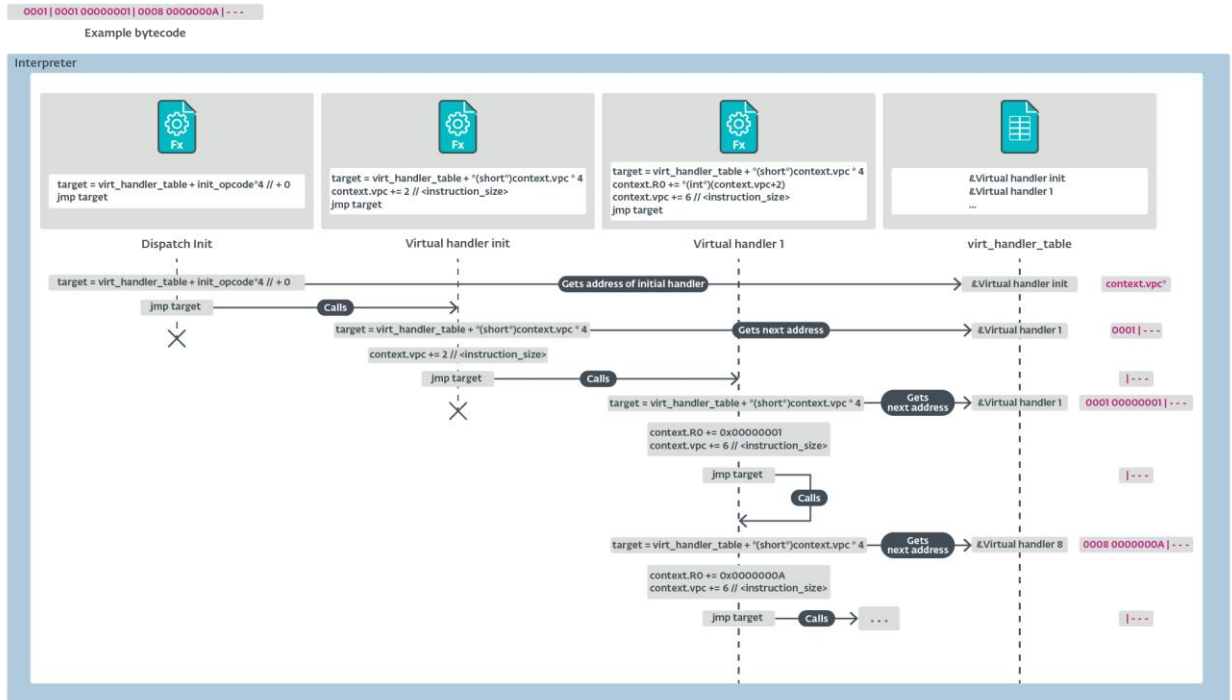


Figure 4. Illustration of Direct Threading

**Obfuscation techniques** are a kind of software protection intended to make code hard to understand and hence conceal its objectives. Such techniques were initially developed to protect the intellectual property of legitimate software, i.e., to hamper reverse engineering.

**Virtual machines used as obfuscation engines** are based on process virtual machines, as described above. The primary difference is that they are not intended to run cross-platform applications and they usually take machine code compiled or assembled for a known ISA, disassemble it and translate that to their own virtual ISA. It is also usually the case that the VM environment and the virtualized application code are contained in one application, whereas traditional process VMs usually consist of a process that runs as a standalone application that loads separate, virtualized applications

The strength of this obfuscation technique resides in the fact that the ISA of the VM is unknown to any prospective reverse engineer – a thorough analysis of the VM, which can be very time-consuming, is required to understand the meaning of the virtual instructions and other structures of the VM. Further, if performance is not an issue, the VM's ISA can be designed to be arbitrarily complex, slowing its execution of virtualized applications, but making

reverse engineering even more complex. Understanding of the VM is necessary for decoding the bytecode and making the virtualized code understandable.

**Context** has a bit of a different meaning in regard to obfuscating virtual machines: each time we want to switch from the native to virtual ISA or vice-versa, sufficient information – context – on the current operating state must be stored so that when the ISA has to be switched back, execution can resume with only the relevant data and registers modified.

Additionally, obfuscating VMs usually virtualize only certain “interesting” functions – native context is mapped to the virtual one and bytecode, representing the respective function, is chosen beforehand. The built-in interpreter is invoked afterwards (Figure 5). Beginnings of the original functions contain code that prepares and executes the interpreter – entry of the VM (`vm_entry`); the rest of their code is omitted in Figure 5.

Interpreter, bytecode, and virtual ISA code with data of obfuscating VMs are often all stored in a dedicated section of the executable binary, along with the rest of the partially virtualized program.

Figure 5 shows the way a function, `Function 1`, in the original application targeting a common ISA can be virtualized for an obfuscating VM’s ISA. It needs to be converted into bytecode, for example using a `generate_bytecode` method. Its body is afterwards overwritten by a call into `vm_entry` and zeroes. The `vm_entry` function chooses the respective bytecode, for example, based on the calling function’s address, then conducts a context switch, and next interprets the bytecode. Finally, it returns to the code where the virtualized function, `Function 1`, would return.

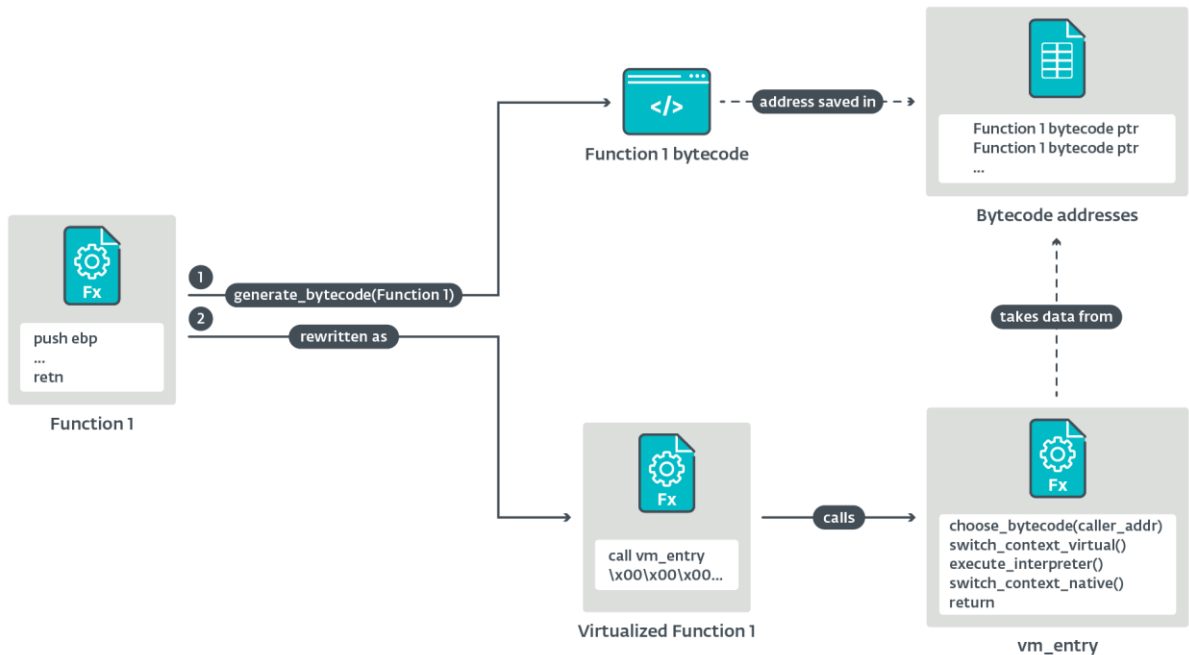


Figure 5. Overview of the virtualization process

In VMs hosted on x86 architectures, such context switches usually consist of a series of PUSH and POP instructions. For example:

```

PUSH EAX
PUSH EBX
PUSH ECX
...
MOV ECX, context_addr
POP DWORD PTR [ECX]
POP DWORD PTR [ECX + 4]
POP DWORD PTR [ECX + 8]
...

```

When the bytecode is fully processed, virtual context is mapped back to native context and execution continues in the non-virtualized code; however, another virtualized function could be executed in the same manner, right away.

Note that several context switches can occur in one virtualized function, for example when a native instruction from the original ISA could not be translated to virtual instructions or an unknown function from the native API needs to be executed.

# 1.1 Documented techniques for deobfuscation of virtual machines

Obfuscating VM techniques have become widely misused for illicit purposes such as obfuscation of malware samples as they hinder both analysis and detection. Hence there is motivation to overcome these obfuscation techniques so as to facilitate analysis of such malicious code and to achieve overall improvement of detection methods.

But first, we want to clarify several terms that are used in this and following sections and might not be known to all readers.

**Symbolic execution** is a code analysis technique, where specific variables are represented with symbolic values instead of concrete data. Arbitrary operations with these symbolic values produce symbolic expressions. It is usually applied on the code's IR and the symbolic expressions include flags.

One can visualize the symbolic expressions like mathematical formulas as can be seen in the following example, where `irb1` contains a block of pseudo-IR:

`irb1:`

`R13 = R13 + 0x027D3930`

`RBX = RCX + 0x05`

`R13 = R13 + -RSI`

`R13 = R13 + RBX`

`irb1_symb:`

`RBX = RCX + 0x05`

`R13 = R13 + RCX + 0x05 + -RSI + 0x027D3930`

`ZF = R13 + RCX + 0x05 + -RSI + 0x027D3930 == 0x00`

`...`

The state of symbolically executed code consists of:

- Values of all variables
- Program counter
- Accumulated constraints that the program's inputs need to satisfy to reach the associated location from the entry point

Accumulated constraints can be understood as a theory in logic. In order to find concrete values of the initial variables with symbolic values – inputs – we need to find a satisfying model, which can be done with an SMT (satisfiability modulo theories) [6] solver.

**Path coverage** is another code analysis technique that determines all possible paths in a piece of code. It is usually implemented using symbolic execution instructed to explore all reachable paths – reachability of newly discovered paths is verified by an SMT solver and already known paths are marked to prevent infinite loops.

Microsoft describes **program synthesis** as “the task of automatically discovering an executable piece of code given user intent expressed using various forms of constraints such as input-output examples, demonstrations, natural language, etc.”. [7]

Several techniques to deal with VM-based obfuscation have been proposed in the past. Here we briefly walk through them and discuss their advantages and disadvantages.

Rolf Rolles described several standard steps to manually recover the original code, where the drawback is time-complexity: [8]

1. Reverse engineer and understand structures of the VM
2. Detect entries into the VM
3. Develop a disassembler for the instruction set by identifying the purpose of individual virtual opcodes or matching them against already known ones
4. Disassemble the bytecode and convert it into intermediate representation – the semantics of some instructions might be hard to comprehend in basic blocks without further translation (e.g., stack-based VMs would contain a lot of confusing `PUSH` and `POP` machinations”)
5. Apply compiler optimizations to get rid of additional obfuscation techniques
6. Generate the deobfuscated code

He additionally suggested the use of pure symbolic execution on the virtual opcodes in the fourth step to obtain a representation, where each opcode is a mathematical function that is a map from its input space into itself. The pure symbolic execution technique was later independently implemented in a Miasm blogpost [9].

Jonathan Salwan, Sébastien Bardin, and Marie-Laure Potet proposed a fully automatic approach to overcome obfuscating VM protection on samples with a finite number of executable paths. The approach consists of the following steps: [10]

1. Identification of the sample’s inputs
2. Isolation of pertinent instructions dependent on the identified inputs on an execution trace
3. Performance of a path coverage analysis to reach new paths – traces

4. Reconstruction of the original program from the resulting traces – they are combined and compiler optimizations partially recover the control flow graph

Tim Blazytko, Moritz Contag, Cornelius Aschermann, and Thorsten Hol produced a semi-automatic approach, based on program synthesis, that uses instruction traces as a black-box oracle to produce random input and output pairs. The I/O pairs are subsequently used to learn the code’s underlying semantics with the synthesizer. [11]

These pairs and semantics are generated for the virtual opcodes that must be identified beforehand – the VM needs to be partially reverse engineered to locate its components.

The approach does not seem to be applicable to some complex (particularly obfuscating) VMs due to its time complexity, as it reportedly took almost three hours to process 36 virtual opcodes of a VM – duplication of handlers, which is a simple and common obfuscation technique, would be a huge issue.

## 1.2 The Miasm framework

Miasm is a free and open-source reverse-engineering framework that aims to analyze, modify and generate binary programs. It has a number of useful features that we use throughout our analysis: [12]

- Opening, modifying and generating binary files – PE and ELF
- Assembling and disassembling of various architectures such as x86, ARM, MIPS...
- Representing assembly semantics using intermediate representation
- Simplification rules for automatic deobfuscation
- Symbolic execution engine
- ...

There are several frameworks for reverse-engineering that provide the features that we needed; we decided to use Miasm in this project simply because it is actively maintained, and we are already familiar and satisfied with it.

The features that we want to use are covered in the example section of its GitHub repository description and its documentation. [13]

Semantics of Miasm’s IR are summarized in

Table *I*, since they are going to be used repeatedly.

Table 1. Miasm’s IR semantics

Element	Example
ExprId	EAX
ExprAssign	A=B
ExprInt	0x18
ExprLoc	location_1
ExprCond	A ? B : C
ExprMem	@16[ESI]
ExprOp	A + B
ExprSlice	AH = EAX[8:16]
ExprCompose	{EAX 0 32, 0x0 32 64}

The destination address of a symbolic execution performed over a block of code is saved in the respective program counter such as RIP and additionally in a special variable IRDst.

Note that during Miasm’s symbolic execution: initial values of registers, which are treated as variables, are symbolic and their format is <register name>\_init. Simplification rules are applied automatically to the symbolic expressions. For example, the symbolic expression  $RAX = RCX + 0x2 + 0x3$  is automatically simplified into  $RAX = RCX\_init + 0x5$ .

## 1.3 Choice of virtual machine

We are going to analyze a VM that is used to protect a sample of a malicious loader called Wslink [14]. The sample does not appear to contain any artifacts that would link it to any known commercial code protection product right away.

However, further analysis revealed that it behaves and contains structures just like VMs generated by CodeVirtualizer (CV) [15], which is a modern and commercial program for code protection, and we assess with high confidence that it is indeed the used obfuscator.

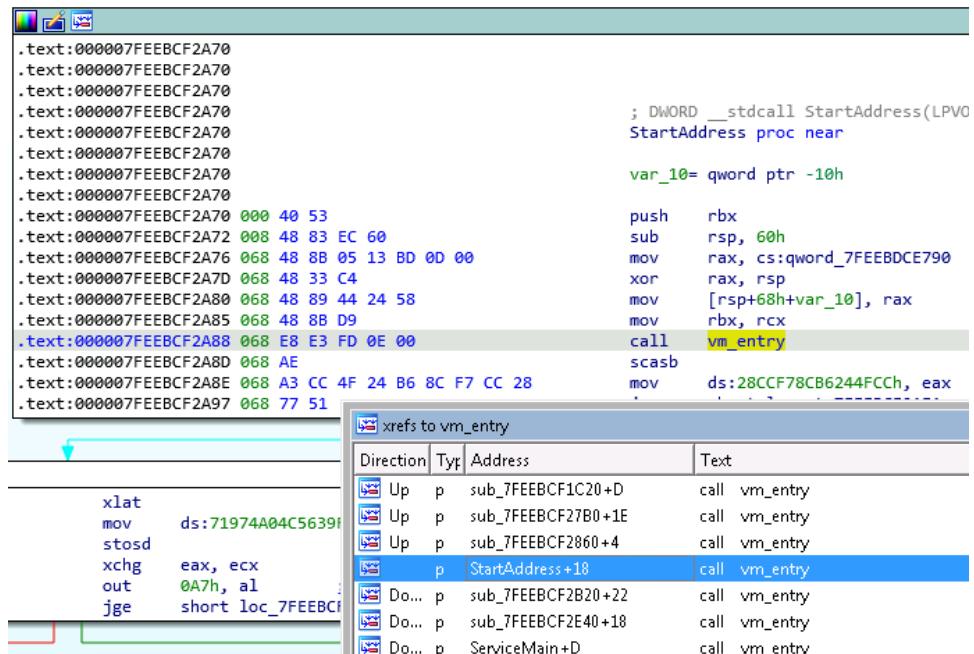
We are going to analyze the applied VM in the rest of the thesis, propose methods to deal with the VM and recover a part of the original code to prove the effectivity of the suggested method.



To conduct the analysis, we decided to use disassembler and decompiler IDA Pro, which is a standard tool in the industry along with reverse-engineering framework Miasm introducing some useful IDA Pro plugins and means to better understand and deobfuscate the code.

## 2 CV's virtual machine entry – vm\_entry

Let's get to the analysis of CV's VM now. There are several function calls that enter the VM, all of which are followed by some gibberish data that IDA attempts to disassemble – the data most likely just overwrites the function's original code before virtualization (Figure 6).



The screenshot shows the IDA Pro interface. The main window displays assembly code for a function. The code consists of several lines of instructions, many of which are overwritten with gibberish data (e.g., 000 40 53, 008 48 83 EC 60). The assembly code includes instructions like `push rbx`, `sub rsp, 60h`, `mov rax, cs:qword_7FEEBDCE790`, `xor rax, rsp`, `mov [rsp+68h+var_10], rax`, `mov rbx, rcx`, `call vm_entry`, `scasb`, and `mov ds:28CCF78CB6244FCCh, eax`. The `call vm_entry` instruction is highlighted in yellow. Below the assembly code, there is a cross-reference table for `vm_entry`. The table has columns for Direction, Type, Address, and Text. The entries are:

Direction	Type	Address	Text
Up	p	sub_7FEEBCF1C20+D	call vm_entry
Up	p	sub_7FEEBCF27B0+1E	call vm_entry
Up	p	sub_7FEEBCF2860+4	call vm_entry
Up	p	StartAddress+18	call vm_entry
Do...	p	sub_7FEEBCF2B20+22	call vm_entry
Do...	p	sub_7FEEBCF2E40+18	call vm_entry
Do...	p	ServiceMain+D	call vm_entry

Figure 6. Entry point to the virtual machine

The `vm_entry` of the VM:

- calculates the actual base address by subtracting the expected relative virtual address from the actual virtual address of a place in the code
- unpacks code and data related to the VM on the first run; it uses the calculated base address to determine the location of the packed VM and destination of the unpacked data
- executes an initialization function – one of the `vm_pre_init()` functions to be described is based on the caller's relative address that is mapped to the respective `vm_pre_init()`

**Packer.** CV's VM is packed with NsPack to reduce the size of the huge executable file; additional obfuscation is probably just a side effect. Similarities between CV's unpacking code and ClamAV's `unpack()` function are clearly visible (Figure 7 and Figure 8). Note that Ghidra has optimized out calculation of the base address.

```

17 vm_pre_init_dispatch = &vm_pre_init_dispatch_table;
18 base = 0x180000000;
19 if (is_packed != 0) {
20     prepare_in_reg_params();
21     if ((*(in_R8 < '\x02') && (0xd < (uint)in_R9) && (c = SEXT14(in_R8[1]), (int)c < 0xe1)) {
22         firstbyte = 0;
23         if (0x2c < (int)c) {
24             firstbyte = c / 0x2d;
25             c = c % 0x2d;
26         }
27         allocsz = 0;
28         if (8 < (int)c) {
29             allocsz = c / 9;
30             c = c % 9;
31         }
32         very_real_unpack(in_R8 + in_R9, (0x300 << ((char)allocsz + (char)c & 0xfU)) * 2 + 0xe6c, c,
33             allocsz, firstbyte, in_R8 + 0xe, (uint)in_R9 - 0xe, in_RCX, *in_RDX,
34             register0x00000020);
35         *in_RDX = ret_addr;
36         uVar1 = 0;
37     }
38     else {
39         uVar1 = 0xffffffff;
40     }
41     return uVar1;
42 }
43
44 /* choose vm_pre_init() function */
45 while (*vm_pre_init_dispatch != ret_addr + 0x7fffffff) {
46     vm_pre_init_dispatch = vm_pre_init_dispatch + 2;
47 }

```

Figure 7. A part of `vm_entry` of the virtual machine decompiled with Ghidra

```

..if (c>=0xe1) return 1;

..if (c>=0x2d) {
...firstbyte = i = c/0x2d;
...do {c+=0xd3;} while (--i);
..} else firstbyte = 0;

..if (c>=9) {
...allocsz = i = c/9;
...do {c+=0xf7;} while (--i);
..} else allocsz = 0;
..
..tre = c;
..i = allocsz;
..c = (tre+i)&0xff;
..tablesz = ((0x300<<c)+0x736)*sizeof(uint16_t);

..if(cli_checklimits("nspack", ctx, tablesz, 0, 0) !=CL_CLEAN)
...return 1; /* Should be ~15KB, if it's so big it's prolly just not nspacked */
...
..cli_dbgmsg("unsp: table size = %d\n", tablesz);
..if (!(table = cli_malloc(tablesz))) {
...cli_dbgmsg("unspack: Unable to allocate memory for table\n");
...return 1;
..}
..
..dsz = cli_readint32(start_of_stuff+9);
..ssz = cli_readint32(start_of_stuff+5);
..if (ssz <= 13) {
..free(table);
..return 1;
..}

..tre = very_real_unpack(table, tablesz, tre, allocsz, firstbyte, src, ssz, dst, dsz);

```

Figure 8. Function used to unpack `NsPack` in `ClamAV`

The `vm_pre_init_dispatch_table` in Figure 7 is the structure that maps callers' addresses of the `vm_entry` to the respective `vm_pre_init()` functions that are to be described.

**Junk code.** Each part of the unpacked VM is obfuscated with lots of junk code – unnecessary additional instructions significantly decreasing readability of the code. It often uses instruction pairs with opposite effects.

Neither the IDA nor the Ghidra decompiler is able to deal with such obfuscation; however, Miasm's symbolic execution was able to make the code easily readable (Figure 9).

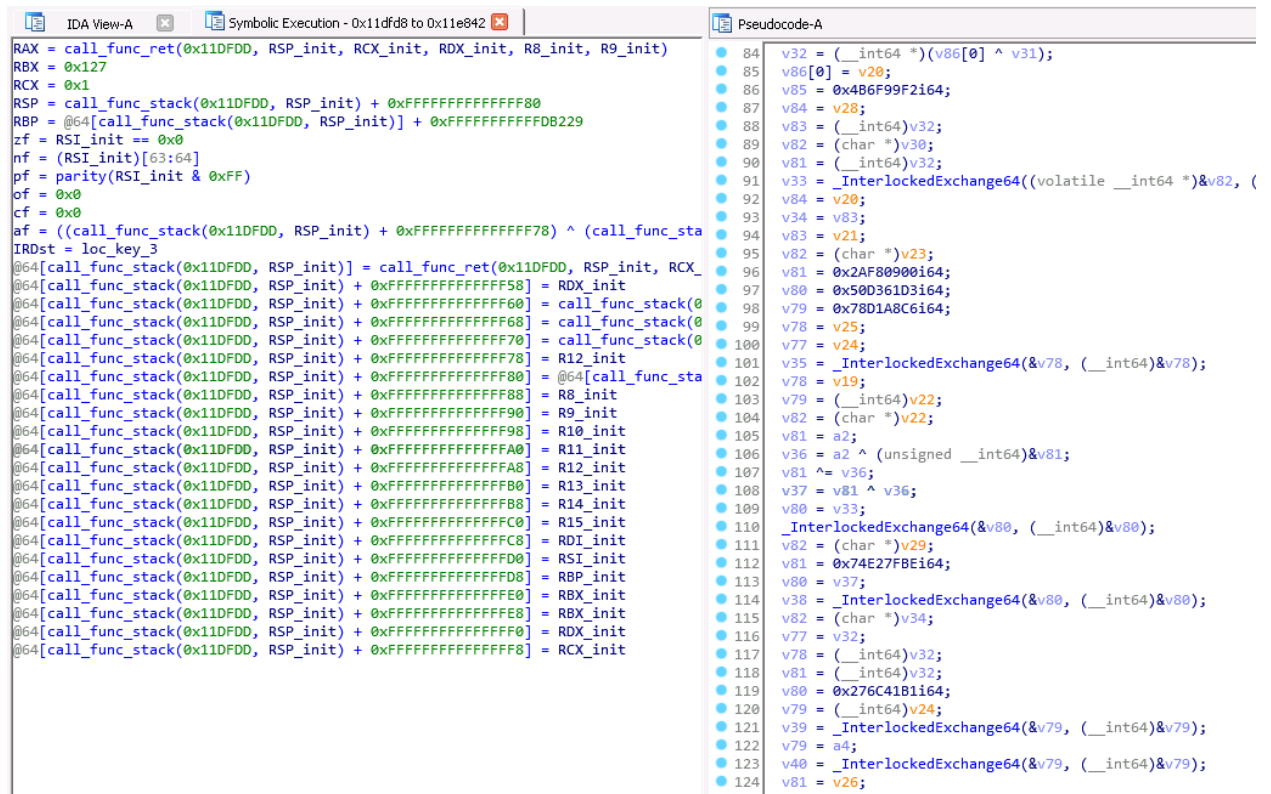


Figure 9. A block of code in Miasm's symbolic execution (left) and a part of the same block in IDA's decompiler (right)

### 3 Virtual machine initialization

Initialization of the VM consists of several steps, such as saving values of the native registers on the stack and later moving them to the virtual context, relocation of its internal structures, or preparation of bytecode. We cover these steps more thoroughly in this chapter.

`vm_pre_init()` functions are meant only to prepare parameters for another stage of initialization (Figure 10). These functions call a single `vm_init()` function (explained in the next section) with specific parameters. The supplied parameters are:

- CPU flags, `RFLAGS`, which are stored on the stack with a `PUSHF` instruction at the beginning of each function
- hardcoded offset to a virtual instruction table that represents the first virtual instruction to be executed (its opcode)
- hardcoded address of the bytecode to be interpreted

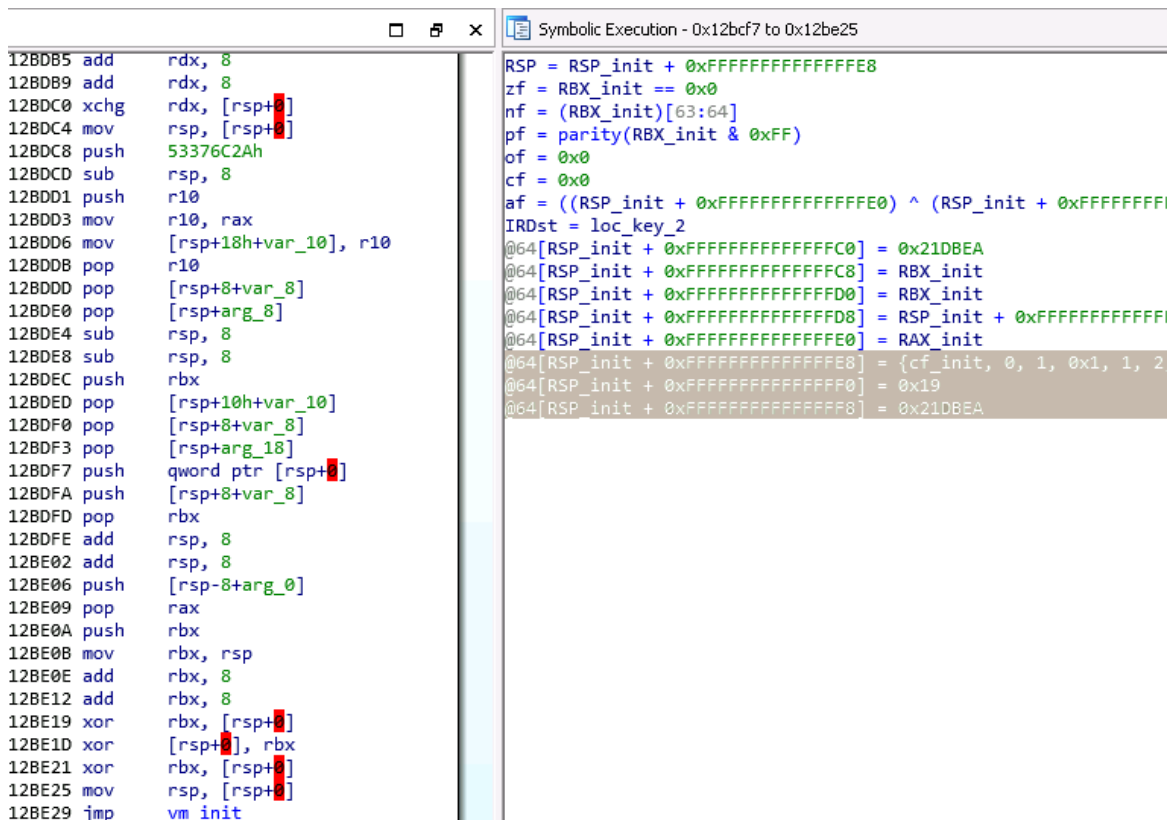


Figure 10. Miasm's symbolic execution of a `vm_pre_init()` showing parameters supplied to `vm_init()`

`vm_init()` pushes all the native registers and the supplied CPU flags from parameters (context) onto the stack; one can actually see it in Figure 9. The native context will later be moved to the virtual one that, in addition, holds several internal registers.

One of the internal registers determines whether another instance of the VM is already running – there is only one global virtual context and only one instance of the VM can run at a time. Figure 11 shows the part of the code busy-waiting for the virtual register, where `RBP` contains the address of the virtual context and `RBX` the offset of the virtual register – the internal register is stored in `[RBX + RBP]`.

The entire function is summarized in Figure 12.

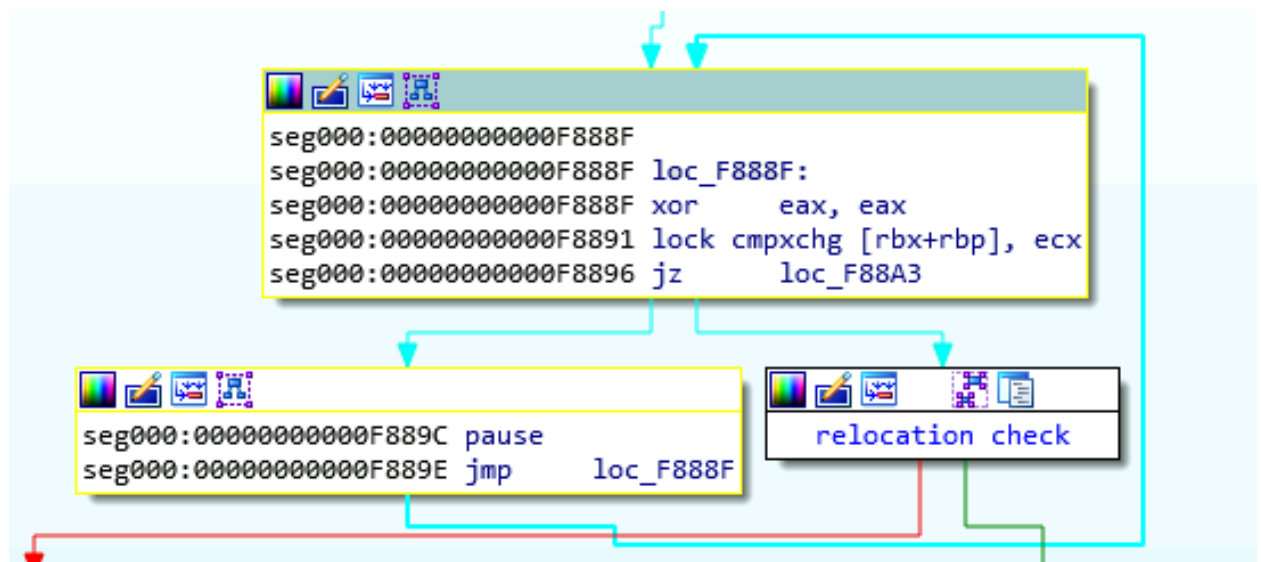


Figure 11. Busy-waiting for interpreter in `vm_init()`

The bytecode's address, supplied in the parameters, is added to the virtual context along with the address of the virtual instruction table, which is hardcoded. Both have a dedicated virtual register.

The VM calculates the base address again in the same way as was described for `vm_entry`; in addition, it stores the address in another internal register that is used later, should an API be called. Then the base address is used to relocate the instruction table, its entries, and the bytecode's address.

The calculated base address is simply added to all the function addresses if they have not already been relocated.

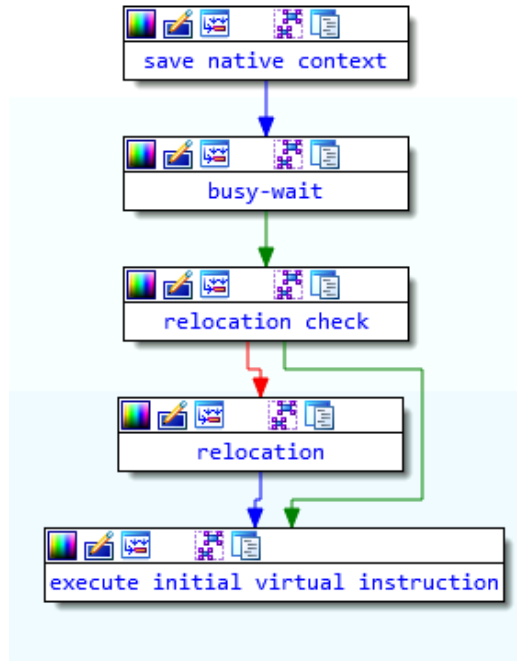


Figure 12. `vm_init()` summary

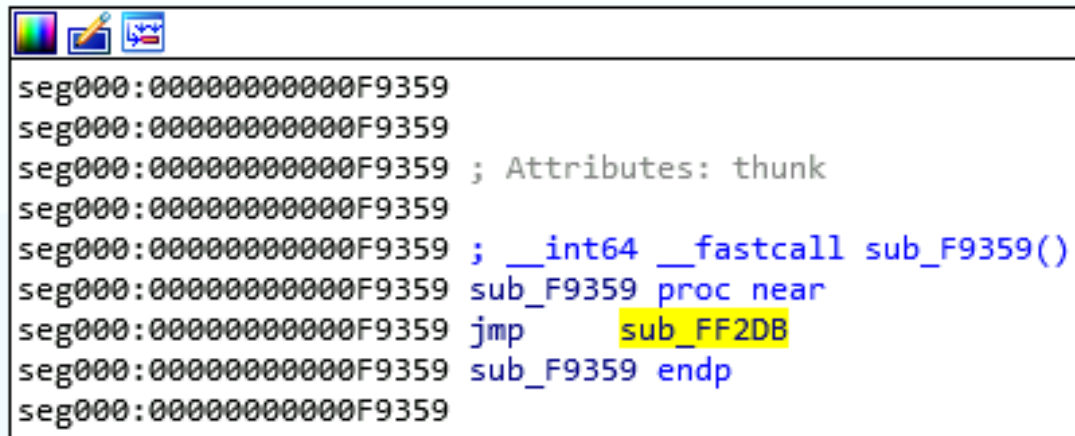
## 4 Virtual instructions

There are only 45 instructions in the virtual instruction table (Figure 13).

```
seg000:000000000011DE70      dq 1EC74Eh, 1EC84Ch, 1EC8F1h, 1ECD73h, 1ECDDEh, 1ECE56h
seg000:000000000011DE70      dq 1ECF4Eh, 1ECFFEh, 1ED1A2h, 1ED343h, 1ED4B1h, 1ED566h
seg000:000000000011DE70      dq 1ED6C9h, 1ED7BFh, 1ED868h, 1ED9A8h, 1EDA1Ah, 1EDF3Ch
seg000:000000000011DE70      dq 1EE042h, 1EE0BAh, 1EE1BAh, 1EE250h, 1EE34Ch, 1EE4A8h
seg000:000000000011DE70      dq 1EE64Fh, 1EE801h, 1EE85Dh, 1EECD4h, 1EEE3Dh, 1EF58Ah
seg000:000000000011DE70      dq 1F0947h, 1F0A87h, 1F0C77h, 1F0E15h, 1F0FC6h, 1F1166h
seg000:000000000011DE70      dq 1F11E6h, 1F13CCh, 1F1570h, 1F1722h, 1F17DFh, 1F186Eh
seg000:000000000011DE70      dq 1F1969h, 1F1A68h, 1F20BFh
```

Figure 13. Virtual instruction table

Let us look at the first one in the table. Initially, we need to relocate it; our dump of the VM starts at address  $0x00$  and it is expected to be at  $base + 0x0F33F5$ , so the target address is  $0x1EC74E - 0x0F33F5$ , which is  $0x0F9359$  (Figure 14).



```
seg000:0000000000F9359
seg000:0000000000F9359
seg000:0000000000F9359 ; Attributes: thunk
seg000:0000000000F9359 ; __int64 __fastcall sub_F9359()
seg000:0000000000F9359 sub_F9359 proc near
seg000:0000000000F9359 jmp sub_FF2DB
seg000:0000000000F9359 sub_F9359 endp
seg000:0000000000F9359
```

Figure 14. The first virtual instruction in the table

The JMP in Figure 14 leads us to a function at  $0x0FF2DB$  whose behavior is remarkably similar to `vm_pre_init()` (Figure 15 and Figure 16 for comparison). The function appears to be pushing another bytecode address, the opcode of the initial virtual instruction, and CPU flags.



```

12BD85 add    rdx, 8
12BD89 add    rdx, 8
12BDC0 xchg  rdx, [rsp+0]
12BDC4 mov    rsp, [rsp+0]
12BDC8 push  53376C2Ah
12BDCD sub    rsp, 8
12BDD1 push  r10
12BDD3 mov    r10, rax
12BDD6 mov    [rsp+18h+var_10], r10
12BDD8 pop    r10
12BDDD pop    [rsp+8+var_8]
12BDE0 pop    [rsp+arg_8]
12BDE4 sub    rsp, 8
12BDE8 sub    rsp, 8
12BDEC push  rbx
12BDED pop    [rsp+10h+var_10]
12BDF0 pop    [rsp+8+var_8]
12BDF3 pop    [rsp+arg_18]
12BDF7 push  qword ptr [rsp+0]
12BDF9 push  [rsp+8+var_8]
12BDFD pop    rbx
12BDFE add    rsp, 8
12BE02 add    rsp, 8
12BE06 push  [rsp-8+arg_0]
12BE09 pop    rax
12BE0A push  rbx
12BE0B mov    rbx, rsp
12BE0E add    rbx, 8
12BE12 add    rbx, 8
12BE19 xor    rbx, [rsp+0]
12BE1D xor    [rsp+0], rbx
12BE21 xor    rbx, [rsp+0]
12BE25 mov    rsp, [rsp+0]
12BE29 jmp    vm_init

```

```

Symbolic Execution - 0x12bcf7 to 0x12be25
RSP = RSP_init + 0xFFFFFFFFFFFFFFE8
zf = RBX_init == 0x0
nf = (RBX_init)[63:64]
pf = parity(RBX_init & 0xFF)
of = 0x0
cf = 0x0
af = ((RSP_init + 0xFFFFFFFFFFFFFFE0) ^ (RSP_init + 0xFFFFFFFF
IRDst = loc_key_2
@64[RSP_init + 0xFFFFFFFFFFFFFFC0] = 0x21DBEA
@64[RSP_init + 0xFFFFFFFFFFFFFFC8] = RBX_init
@64[RSP_init + 0xFFFFFFFFFFFFFFD0] = RBX_init
@64[RSP_init + 0xFFFFFFFFFFFFFFD8] = RSP_init + 0xFFFFFFFF
@64[RSP_init + 0xFFFFFFFFFFFFFFE0] = RAX_init
@64[RSP_init + 0xFFFFFFFFFFFFFFE8] = {cf_init, 0, 1, 0x1, 1, 2
@64[RSP_init + 0xFFFFFFFFFFFFFFF0] = 0x19
@64[RSP_init + 0xFFFFFFFFFFFFFFF8] = 0x21DBEA

```

Figure 15. One of the `vm_pre_init()` functions

```

0xFF3F2 mov    rdi, rax
0xFF3F5 pop    rax
0xFF3F6 push   rdi
0xFF3F7 pop    [rsp+18h+arg_8]
0xFF3FB pop    rdi
0xFF3FC push   [rsp+10h+var_10]
0xFF3FF mov    rbx, [rsp+18h+var_18]
0xFF403 add    rsp, 8
0xFF40A add    rsp, 8
0xFF40E push   [rsp+8+var_8]
0xFF411 push   [rsp+10h+var_10]
0xFF414 mov    rax, [rsp+18h+var_18]
0xFF418 add    rsp, 8
0xFF41F add    rsp, 8
0xFF423 add    rsp, 8
0xFF427 jmp    sub_FF7FFF
0xFF427 sub_FF2DB endp

```

```

Symbolic Execution - 0xff2db to 0xff423
RSP = RSP_init + 0xFFFFFFFFFFFFFFE8
zf = RSP_init == 0x18
nf = (RSP_init + 0xFFFFFFFFFFFFFFE8)[63:64]
pf = parity((RSP_init + 0xFFFFFFFFFFFFFFE8) & 0xFF)
of = (((RSP_init + 0xFFFFFFFFFFFFFFE0) ^ (RSP_init +
cf = (((RSP_init + 0xFFFFFFFFFFFFFFE0) ^ (RSP_init
af = ((RSP_init + 0xFFFFFFFFFFFFFFE0) ^ (RSP_init +
IRDst = loc_key_2
@64[RSP_init + 0xFFFFFFFFFFFFFFC0] = R15_init
@64[RSP_init + 0xFFFFFFFFFFFFFFC8] = 0x1F2189
@64[RSP_init + 0xFFFFFFFFFFFFFFD0] = RAX_init
@64[RSP_init + 0xFFFFFFFFFFFFFFD8] = RAX_init
@64[RSP_init + 0xFFFFFFFFFFFFFFE0] = RAX_init
@64[RSP_init + 0xFFFFFFFFFFFFFFE8] = {cf_init, 0, 1,
@64[RSP_init + 0xFFFFFFFFFFFFFFF0] = 0x3F1
@64[RSP_init + 0xFFFFFFFFFFFFFFF8] = 0x1F2189

```

Figure 16. Miasm's symbolic execution of the first virtual instruction (function at `0x0FF2DB`)

Inspecting the function at `0x0F7FFF` (Figure 17), into which our virtual instruction jumps, reveals that it appears to be another `vm_init()` (Figure 18). When we compare it to

the previous one, we can see that their behaviors are, indeed, the same. We will refer to these functions simply as `vm2_pre_init()` and `vm2_init()`.

```

Symbolic Execution - 0xf7fff to 0xf888b
RAX = call_func_ret(0xF8004, RSP_init, RCX_init, RDX_init, R8_init, R9_init)
RBX = 0xFF
RCX = 0x1
RSP = call_func_stack(0xF8004, RSP_init) + 0xFFFFFFFFFFFFFFF80
RBP = @64[call_func_stack(0xF8004, RSP_init)] + 0xFFFFFFFFFFFFFFF07FFC
zf = call_func_stack(0xF8004, RSP_init) == 0x80
nf = (call_func_stack(0xF8004, RSP_init) + 0xFFFFFFFFFFFFFFF80)[63:64]
pf = parity((call_func_stack(0xF8004, RSP_init) + 0xFFFFFFFFFFFFFFF80) & 0xFF)
of = (((call_func_stack(0xF8004, RSP_init) + 0xFFFFFFFFFFFFFFF78) ^ (call_func_
cf = (((call_func_stack(0xF8004, RSP_init) + 0xFFFFFFFFFFFFFFF78) ^ (call_func_
af = ((call_func_stack(0xF8004, RSP_init) + 0xFFFFFFFFFFFFFFF78) ^ (call_func_s
IRDst = loc_key_3
@64[call_func_stack(0xF8004, RSP_init)] = call_func_ret(0xF8004, RSP_init, RCX
@64[call_func_stack(0xF8004, RSP_init) + 0xFFFFFFFFFFFFFFF60] = @64[call_func_s
@64[call_func_stack(0xF8004, RSP_init) + 0xFFFFFFFFFFFFFFF68] = RDI_init
@64[call_func_stack(0xF8004, RSP_init) + 0xFFFFFFFFFFFFFFF70] = RSI_init
@64[call_func_stack(0xF8004, RSP_init) + 0xFFFFFFFFFFFFFFF78] = RSI_init
@64[call_func_stack(0xF8004, RSP_init) + 0xFFFFFFFFFFFFFFF80] = @64[call_func_s
@64[call_func_stack(0xF8004, RSP_init) + 0xFFFFFFFFFFFFFFF88] = R8_init
@64[call_func_stack(0xF8004, RSP_init) + 0xFFFFFFFFFFFFFFF90] = R9_init
@64[call_func_stack(0xF8004, RSP_init) + 0xFFFFFFFFFFFFFFF98] = R10_init
@64[call_func_stack(0xF8004, RSP_init) + 0xFFFFFFFFFFFFFFFA0] = R11_init
@64[call_func_stack(0xF8004, RSP_init) + 0xFFFFFFFFFFFFFFFA8] = R12_init
@64[call_func_stack(0xF8004, RSP_init) + 0xFFFFFFFFFFFFFFFB0] = R13_init
@64[call_func_stack(0xF8004, RSP_init) + 0xFFFFFFFFFFFFFFFB8] = R14_init
@64[call_func_stack(0xF8004, RSP_init) + 0xFFFFFFFFFFFFFFFC0] = R15_init
@64[call_func_stack(0xF8004, RSP_init) + 0xFFFFFFFFFFFFFFFC8] = RDI_init
@64[call_func_stack(0xF8004, RSP_init) + 0xFFFFFFFFFFFFFFFD0] = RSI_init
@64[call_func_stack(0xF8004, RSP_init) + 0xFFFFFFFFFFFFFFFD8] = RBP_init
@64[call_func_stack(0xF8004, RSP_init) + 0xFFFFFFFFFFFFFFFE0] = RBX_init
@64[call_func_stack(0xF8004, RSP_init) + 0xFFFFFFFFFFFFFFFE8] = RDX_init
@64[call_func_stack(0xF8004, RSP_init) + 0xFFFFFFFFFFFFFFFF0] = RDX_init
@64[call_func_stack(0xF8004, RSP_init) + 0xFFFFFFFFFFFFFFFF8] = RCX_init

```

Figure 17. Miasm's symbolic execution of the first block of `vm2_init()`

```

IDA View-A | Symbolic Execution - 0x11df8 to 0x11e842 | Pseudocode-A

RAX = call_func_ret(0x11DFDD, RSP_init, RCX_init, RDX_init, R8_init, R9_init)
RBX = 0x127
RCX = 0x1
RSP = call_func_stack(0x11DFDD, RSP_init) + 0xFFFFFFFFFFFFF80
RBP = @64[call_func_stack(0x11DFDD, RSP_init)] + 0xFFFFFFFFFFDB229
zf = RSI_init == 0x0
nf = (RSI_init)[63:64]
pf = parity(RSI_init & 0xFF)
of = 0x0
cf = 0x0
af = ((call_func_stack(0x11DFDD, RSP_init) + 0xFFFFFFFFFFFFF78) ^ (call_func_sta
IRDst = loc_key_3
@64[call_func_stack(0x11DFDD, RSP_init)] = call_func_ret(0x11DFDD, RSP_init, RCX_
@64[call_func_stack(0x11DFDD, RSP_init) + 0xFFFFFFFFFFFFF58] = RDX_init
@64[call_func_stack(0x11DFDD, RSP_init) + 0xFFFFFFFFFFFFF60] = call_func_stack(0
@64[call_func_stack(0x11DFDD, RSP_init) + 0xFFFFFFFFFFFFF68] = call_func_stack(0
@64[call_func_stack(0x11DFDD, RSP_init) + 0xFFFFFFFFFFFFF70] = call_func_stack(0
@64[call_func_stack(0x11DFDD, RSP_init) + 0xFFFFFFFFFFFFF78] = R12_init
@64[call_func_stack(0x11DFDD, RSP_init) + 0xFFFFFFFFFFFFF80] = @64[call_func_sta
@64[call_func_stack(0x11DFDD, RSP_init) + 0xFFFFFFFFFFFFF88] = R8_init
@64[call_func_stack(0x11DFDD, RSP_init) + 0xFFFFFFFFFFFFF90] = R9_init
@64[call_func_stack(0x11DFDD, RSP_init) + 0xFFFFFFFFFFFFF98] = R10_init
@64[call_func_stack(0x11DFDD, RSP_init) + 0xFFFFFFFFFFFFFA0] = R11_init
@64[call_func_stack(0x11DFDD, RSP_init) + 0xFFFFFFFFFFFFFA8] = R12_init
@64[call_func_stack(0x11DFDD, RSP_init) + 0xFFFFFFFFFFFFFB0] = R13_init
@64[call_func_stack(0x11DFDD, RSP_init) + 0xFFFFFFFFFFFFFB8] = R14_init
@64[call_func_stack(0x11DFDD, RSP_init) + 0xFFFFFFFFFFFFFC0] = R15_init
@64[call_func_stack(0x11DFDD, RSP_init) + 0xFFFFFFFFFFFFFC8] = RDI_init
@64[call_func_stack(0x11DFDD, RSP_init) + 0xFFFFFFFFFFFFFD0] = RSI_init
@64[call_func_stack(0x11DFDD, RSP_init) + 0xFFFFFFFFFFFFFD8] = RBP_init
@64[call_func_stack(0x11DFDD, RSP_init) + 0xFFFFFFFFFFFFFE0] = RBX_init
@64[call_func_stack(0x11DFDD, RSP_init) + 0xFFFFFFFFFFFFFE8] = RBX_init
@64[call_func_stack(0x11DFDD, RSP_init) + 0xFFFFFFFFFFFFFE0] = RDX_init
@64[call_func_stack(0x11DFDD, RSP_init) + 0xFFFFFFFFFFFFFE8] = RCX_init

v32 = (__int64 *) (v86[0] ^ v31);
v86[0] = v20;
v85 = 0x4B6F99F2i64;
v84 = v28;
v83 = (__int64)v32;
v82 = (char *)v30;
v81 = (__int64)v32;
v33 = _InterlockedExchange64((volatile __int64 *)&v82, (
v84 = v20;
v34 = v83;
v83 = v21;
v82 = (char *)v23;
v81 = 0x2AF80900i64;
v80 = 0x50D361D3i64;
v79 = 0x78D1A8C6i64;
v78 = v25;
v77 = v24;
v35 = _InterlockedExchange64(&v78, (__int64)&v78);
v78 = v19;
v79 = (__int64)v22;
v82 = (char *)v22;
v81 = a2;
v36 = a2 ^ (unsigned __int64)&v81;
v81 ^= v36;
v37 = v81 ^ v36;
v80 = v33;
_InterlockedExchange64(&v80, (__int64)&v80);
v82 = (char *)v29;
v81 = 0x74E27FBEi64;
v80 = v37;
v38 = _InterlockedExchange64(&v80, (__int64)&v80);
v82 = (char *)v34;
v77 = v32;
v78 = (__int64)v32;
v81 = (__int64)v32;
v80 = 0x276C41B1i64;
v79 = (__int64)v24;
v39 = _InterlockedExchange64(&v79, (__int64)&v79);
v79 = a4;
v40 = _InterlockedExchange64(&v79, (__int64)&v79);
v81 = v26;

```

Figure 18. Miasm’s symbolic execution of the first block of `vm_init()`

Inspection of the other instructions revealed that they all execute this second VM with different `vm2_pre_init()` functions – this clearly shows that there are two layers of VMs.

Virtual instructions of the first VM execute `vm2_pre_init()` directly without any dispatch table based on the caller’s address. The number of virtual instructions in the second VM is significantly higher – 1071 (Figure 19).

F5E87	dq	0A17D5h,	0A184Ch,	0A1CFDh,	0A214Dh,	0A2573h,	0A292Eh
F5E87	dq	0A2CCCh,	0A30F0h,	0A355Ah,	0A3827h,	0A3BF7h,	0A3F8Ah
F5E87	dq	0A43B1h,	0A4771h,	0A4AA5h,	0A4EBDh,	0A5070h,	0A54E7h
F5E87	dq	0A586Eh,	0A595Bh,	0A5D89h,	0A5EE2h,	0A626Ah,	0A6639h
F5E87	dq	0A6A34h,	0A6D40h,	0A70E7h,	0A7565h,	0A794Ch,	0A7CDCh
F5E87	dq	0A81F0h,	0A86A5h,	0A89CDh,	0A8A41h,	0A8E01h,	0A9194h
F5E87	dq	0A9594h,	0A99CFh,	0A9E35h,	0AA279h,	0AA641h,	0AA93Eh
F5E87	dq	0AABB6h,	0AAF82h,	0AB354h,	0AB736h,	0ABB31h,	0ABD6Bh
F5E87	dq	0AC222h,	0AC433h,	0AC78Eh,	0ACB51h,	0ACF28h,	0AD2D0h
F5E87	dq	0AD62Fh,	0AD919h,	0ADDE6h,	0AE213h,	0AE608h,	0AE8D0h
F5E87	dq	0AEC5h,	0AF0A8h,	0AF585h,	0AF921h,	0AFC90h,	0B004Ch
F5E87	dq	0B041Eh,	0B0725h,	0B0AD9h,	0B0CCCh,	0B10A8h,	0B153Fh
F5E87	dq	0B194Ah,	0B1D1Eh,	0B20C5h,	0B2396h,	0B284Dh,	0B2C39h
F5E87	dq	0B3074h,	0B34F9h,	0B3844h,	0B3C61h,	0B4010h,	0B4399h
F5E87	dq	0B46E9h,	0B4795h,	0B4A14h,	0B4D97h,	0B511Bh,	0B559Ah
F5E87	dq	0B57EEh,	0B5AF8h,	0B5DECh,	0B61E2h,	0B65E1h,	0B6AFBh
F5E87	dq	0B757Eh,	0B7876h,	0B7C07h,	0B7F98h,	0B8322h,	0B864Eh
F5E87	dq	0B8944h,	0B8D39h,	0B903Dh,	0B9430h,	0B986Eh,	0B9C46h
F5E87	dq	0B9E44h,	0BA14Ah,	0BA5C9h,	0BA948h,	0BAE88h,	0BB32Bh
F5E87	dq	0BB7D3h,	0BBBE3h,	0BBFC1h,	0BC3BCh,	0BC7D6h,	0BCB70h
F5E87	dq	0BD05Fh,	0BD498h,	0BD6DFh,	0BDAA7h,	0BDEF9h,	0BE2C4h
F5E87	dq	0BE705h,	0BEB00h,	0BEBB2h,	0BEF4Bh,	0BF2DFh,	0BF607h
F5E87	dq	0BFA9Eh,	0BFE92h,	0C01B0h,	0C05D3h,	0C0AAFh,	0C0E1Ch
F5E87	dq	0C1322h,	0C1750h,	0C1B08h,	0C1E72h,	0C20BCh,	0C23B4h
F5E87	dq	0C26C3h,	0C2A23h,	0C2DF4h,	0C317Ch,	0C3544h,	0C38FDh
F5E87	dq	0C3D25h,	0C4208h,	0C46CBh,	0C4B20h,	0C4E25h,	0C51A5h
F5E87	dq	0C56CEh,	0C5A88h,	0C5E2Ch,	0C61CCh,	0C65F6h,	0C6A31h
F5E87	dq	0C6DB3h,	0C7185h,	0C74A7h,	0C75FFh,	0C7A3Ch,	0C7CBCh
F5E87	dq	0C8063h,	0C82A7h,	0C85EEh,	0C8800h,	0C8C16h,	0C9064h
F5E87	dq	0C9584h,	0C9A0Bh,	0C9E53h,	0CA152h,	0CA4AEh,	0CA855h

Figure 19. A part of the second virtual instruction table

## 4.1 Virtual instructions of the second virtual machine

We start by looking at the first few executed virtual instructions to observe the behavior of the second VM and then try to process the rest of them in a partially automated way.

The diagram in Figure 20 highlights with blue, where the virtual instructions of the second VM are in the structure of the VMs.

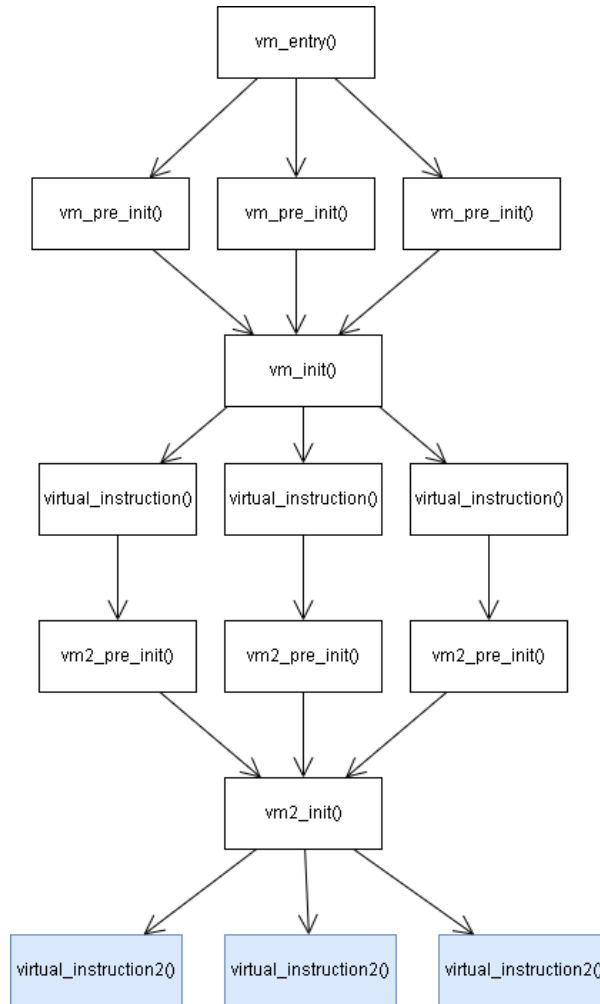


Figure 20. Virtual instructions in the structure of the virtual machines

**The first virtual instruction** is, exceptionally, not obfuscated, as can be seen in Figure 21. Finally, we can see some operations in the virtual context.

By inspecting the modified memory and calculated destination address of the instruction, it is clear that the instruction does three things:

1. Zeroes out a virtual 32-bit register at offset  $0xB5$  in the virtual context (highlighted in gray in Figure 21), which is stored in the RBP register.
2. A virtual 64-bit register at offset  $0x28$  is increased by  $0x04$ : it is the pointer to the bytecode – virtual program counter. The size of the virtual instruction is hence four bytes (highlighted in red in Figure 21).
3. The next virtual instruction is prepared to be executed, the offset to the virtual instruction table – virtual opcode – is fetched from the virtual program counter. The virtual

instruction table is at offset 0xA4 (highlighted in green in Figure 21). This means that the VM uses the Direct Threading Dispatch technique.

Figure 21. The initial virtual instruction of the second VM

Note that the size of the next instruction’s opcode is only two bytes and the remaining word is left unused. We can see that it is just a zero when we look at virtual operands (Figure 22). Sizes of the other instructions differ – it is not just padding that preserves the same size for all instructions.

```

00FED94          dw 2CCh          ; Next virtual opcode
00FED96          dw 0             ; Virtual operand

```

Figure 22. Bytecode of the virtual instruction

**The second virtual instruction** does not do anything special; it just zeroes out several virtual registers and jumps to the next instruction (Figure 23).

```

IRDst = @64[@64[RBP_init + 0xA4] + {0x0, 0, 3, @16[@64[RBP_init + 0x28]], 3, 19, 0x0, 19, 64}]
@16[RBP_init + 0xB] = 0x0
@64[RBP_init + 0x28] = @64[RBP_init + 0x28] + 0x2
@32[RBP_init + 0x48] = 0x0
@32[RBP_init + 0x70] = 0x0
@32[RBP_init + 0x94] = 0x0
@32[RBP_init + 0xA0] = 0x0
@32[RBP_init + 0xEE] = 0x0
@32[RBP_init + 0xFA] = 0x0
@16[RBP_init + 0x103] = 0x0
@32[RBP_init + 0x133] = 0x0
@16[RBP_init + 0x149] = 0x0

```

Figure 23. Destination address and memory modified by the second virtual instruction

The **third virtual instruction** stores the address of the stack pointer in a virtual register (Figure 24); the offset of the register is determined by one of the operands, and its offset is  $0 \times 0141$  in our case.

```
IRDst = @64[@64[RBP_init + 0xA4] + {0x0, 0, 3, @16[@64[RBP_init + 0x28] + 0x2], 3, 19, 0x0, 19, 64}]
@64[RBP_init + {@16[@64[RBP_init + 0x28]], 0, 16, 0x0, 16, 64}] = RSP_init
@64[RBP_init + 0x28] = @64[RBP_init + 0x28] + 0x4
```

Figure 24. Destination address and memory modified by the third virtual instruction

The **fourth instruction** contains two immediately visible anomalies in comparison with previous instructions – the stack pointer’s delta is lower at the end of the function and it contains a conditional branch (Figure 25).

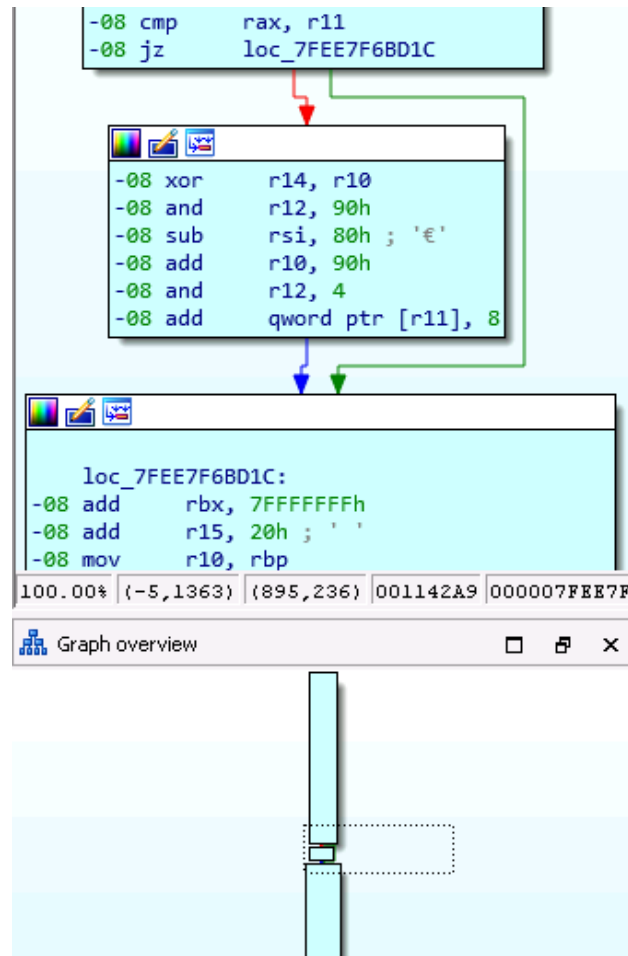


Figure 25. The conditional branch and delta of the stack pointer of the fourth virtual instruction

Symbolic execution of the first block reveals that a value is popped from the stack into a virtual register (Figure 26), which makes sense as the values of the native registers remain on the stack after being saved there by `vm2_init()`. They are now being moved to the virtual context – the context switch is partially performed by a number of virtual instructions, each of which pops one value off the stack into a different register.

```
IRDst = (((@16[RBP_init + 0xB] + -(@32[RBP_init + 0x70] ^ {@16[@64[RBP_init + 0x28] + 0x4], 0, 16, 0x0, 16, 32})[0:16]) ^ 0x3038, 0, 16, 0x0, 16, 64] == {@16[@64[RBP_init + 0x28] + 0x6], 0, 16, 0x0, 16, 64])
@16[RBP_init + 0xB] = @16[RBP_init + 0xB] + -(@32[RBP_init + 0x70] ^ {@16[@64[RBP_init + 0x28] + 0x4], 0, 16, 0x0, 16, 32})[0:16]
@32[RBP_init + 0x70] = @32[RBP_init + 0x70] & (@32[RBP_init + 0x70] ^ {@16[@64[RBP_init + 0x28] + 0x4], 0, 16, 0x0, 16, 32})
@64[RBP_init + (@16[RBP_init + 0xB] + -(@32[RBP_init + 0x70] ^ {@16[@64[RBP_init + 0x28] + 0x4], 0, 16, 0x0, 16, 32})[0:16]) ^ 0x3038, 0, 16, 0x0, 16, 64] = @64[RSP_init]
```

Figure 26. Destination address and memory modified by the fourth virtual instruction

The virtual register, where the value of the native register is to be saved, is determined by an operand and two other virtual registers at offsets `0x0B` and `0x70`. However, their initial value is already known: they were set to zero by the second virtual instruction (Figure 23), which means that we can calculate the offset of the register and simplify the expressions – they are used just to obfuscate the code.

**Rolling decryption.** Analysis of other virtual instructions confirmed that the virtual registers at offsets `0x0B` and `0x70` are meant just to encode operands. This technique is called [rolling decryption](#) and it is known to be used by the [VMProtect](#) obfuscator. However, it is the only overlap with that obfuscator and we are highly confident that this VM is different.

The obfuscation technique is certainly one of the reasons for the enormous number of virtual instructions – use of the technique requires duplication of individual instructions since each uses a different key to decode the operands.

**Simplification.** The expressions can be simplified to the following when we apply the known values of the virtual registers:

```
IRDst = (-@16[@64[RBP_init + 0x28] + 0x4] ^ 0x3038 ==
@16[@64[RBP_init + 0x28] + 0x6])?(0x7FEC91ABD1C,0x7FEC91ABCF6)
@64[RBP_init + {-@16[@64[RBP_init + 0x28] + 0x4] ^ 0x3038, 0,
16, 0x0, 16, 64}] = @64[RSP_init]
```

Now let us take a look at the expression in the conditional block:



```
@64[RBP_init + {@16[@64[RBP_init + 0x28] + 0x6], 0, 16, 0x0,
16, 64}] = @64[RBP_init + {@16[@64[RBP_init + 0x28] + 0x6], 0,
16, 0x0, 16, 64}] + 0x8
```

We can now see that the virtual instruction is definitely POP – it moves a value off the top of the stack to a virtual register, whose offset is still obfuscated with a simple XOR; it additionally increases the stack pointer when the destination register is not the stack pointer.

As values in the bytecode are known too, we can apply them and simplify the instruction even further into the following final unconditional expressions:

```
IRDst = @64[@64[RBP_init + 0xA4] + 0x5A8]
@64[RBP_init + 0x28] = @64[RBP_init + 0x28] + 0x8
@64[RBP_init + 0x141] = @64[RBP_init + 0x141] + 0x8
@64[RBP_init + 0x12A] = @64[RSP_init]
```

**Automating analysis of the virtual instructions.** As doing this for more than 1000 instructions would be very time consuming, we wrote a Python script with Miasm that collects this information for us so we can get a better overview of what is going on. We are particularly interested in modified memory and destination addresses.

Just as in the fourth virtual instruction, we will treat certain virtual registers as concrete values to retrieve clear expressions. These registers are dedicated to the rolling decryption and perform memory accesses that are relative to the bytecode pointer, e.g. [`<obf_reg_1>`] = [`<bytecode_ptr> + 0x05`] ^ 0xABCD.

Subsequently we concretize the pointer to the virtual instruction table too and, by the end of the virtual instruction: calculate addresses of the next ones, clear the symbolic state, and start with the following virtual instructions.

We additionally save aside memory assignments that are not related to the internal registers of the VM and gradually build a graph based on the virtual program counter (Figure 27).

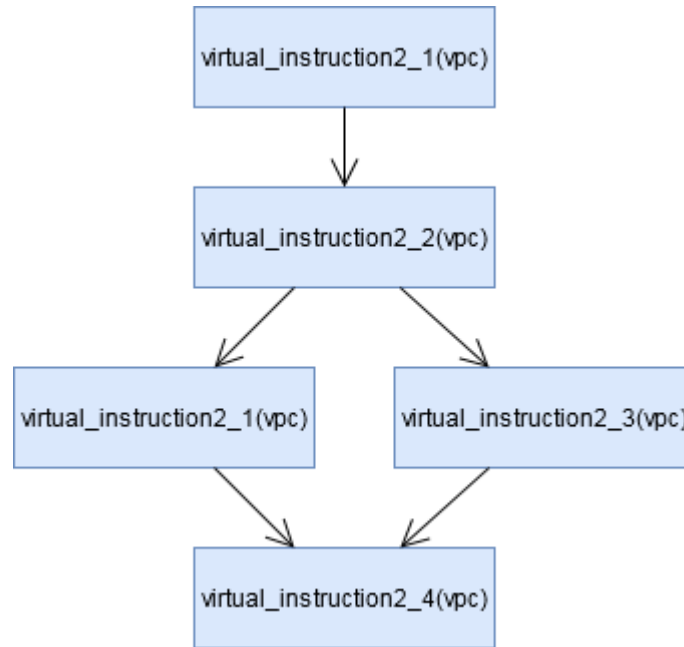


Figure 27. Call graph generated from memory assignments and the VPC

We stop when we cannot unambiguously determine the next virtual instructions to be executed; one can automatically process most of the virtual instructions in this way.

Note that instructions featuring complex loops cannot be processed with certainty and need to be addressed individually due to the path explosion problem of symbolic execution, which is described for example in the paper Demand-Driven Compositional Symbolic Execution [16]: “Systematically executing symbolically all feasible program paths does not scale to large programs. Indeed, the number of feasible paths can be exponential in the program size, or even infinite in presence of loops with unbounded number of iterations.”

**Getting back to the first virtual machine.** Before diving into the virtual instructions of the first VM, let us recap where we currently are. We have just described a way to semiautomate processing of the bytecode belonging to the second VM (blue in Figure 28) that interprets virtual instructions of the first VM (red in Figure 28). Now we move on to inspect instructions of the first VM with this approach.

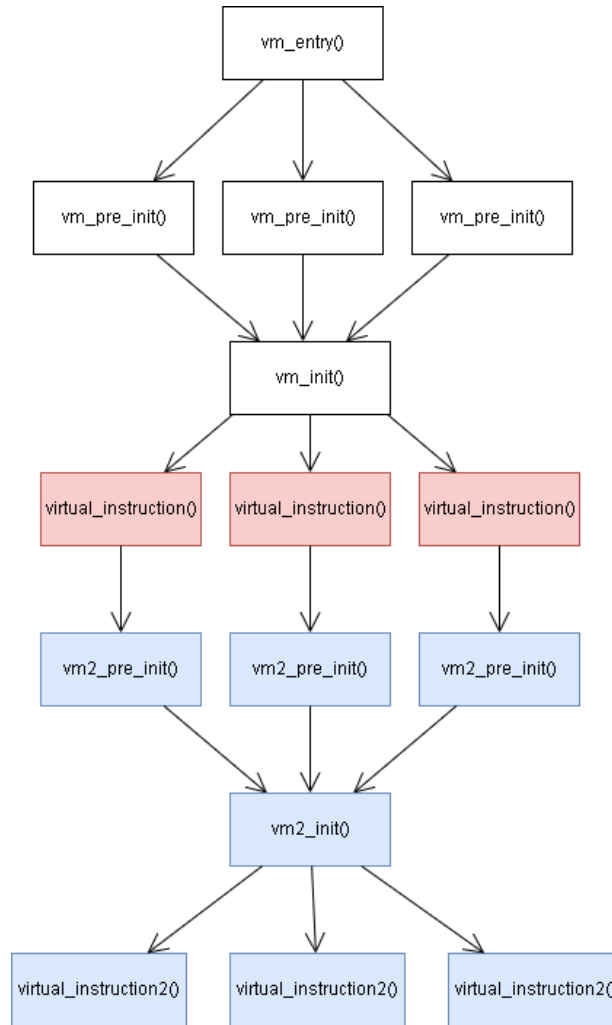


Figure 28. Virtual instructions in the structure of the virtual machines

## 4.2 The initial virtual instruction

In this section we describe the results of processing of the initial virtual instruction of the first VM in the semiautomatic manner that was described in the previous section.

We performed all the processing on a virtual machine with i7-4770 CPU and 4GB of memory. Statistics in Table 2 have been extracted from the processing of the initial virtual instruction.

*Table 2. Statistics of the initial virtual instruction*

Size of the bytecode block in bytes	1,145
Total number of processed virtual instructions	109
Total number of underlying native instructions	17,406
Total number of resulting IR instructions (including IRDsts)	307
Execution time in seconds	10.6509

The resulting control flow graph built out of the semantics extracted from the virtual instructions of the second VM's bytecode that interprets the initial virtual instruction from the first VM can be seen in Figure 29. We can divide the series into a few parts.

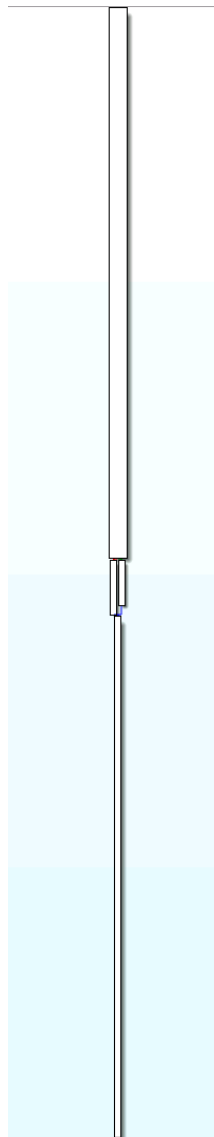


*Figure 29. Control flow graph of the initial virtual instruction*

**Prologue.** As expected, the graph starts with a series of POP instructions that move values of the native registers saved beforehand in `vm2_init()` to the virtual ones (Figure 30). To determine positions of the native registers on the stack, we could symbolically evaluate the first block of `vm2_init()` and map the virtual registers to their native versions, which would make the code easier to read, but that is not important now.

Remember that the virtual register at offset `0x1E` contains the stack pointer, and that a POP instruction moves a value off the top of the stack and usually increases the stack pointer.

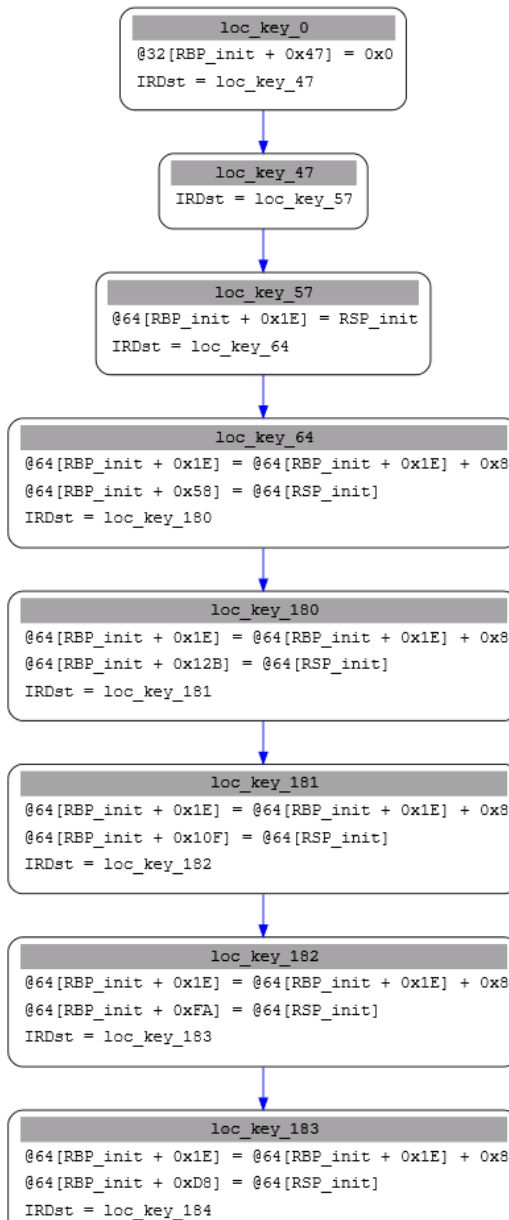


Figure 30. Beginning of the prologue finishing context switch of the second VM

**Epilogue.** To map the virtual registers back to the native ones, the second VM pushes them all onto the stack and then subsequently pops them off one by one to the native ones. Note that we set up an exclusion in our algorithm and disabled optimizations to show assignments to registers in the last virtual instruction (Figure 31).

```

R10 = @64[RSP_init + 0x10]      . . .
R11 = @64[RSP_init + 0x18]
R12 = @64[RSP_init + 0x20]
R13 = @64[RSP_init + 0x28]
R14 = @64[RSP_init + 0x30]
R15 = @64[RSP_init + 0x38]
zf = @32[RSP_init + 0x78][6:7]
nf = @32[RSP_init + 0x78][7:8]
pf = @32[RSP_init + 0x78][2:3]
of = @32[RSP_init + 0x78][11:12]
cf = @32[RSP_init + 0x78][0:1]
af = @32[RSP_init + 0x78][4:5]
df = @32[RSP_init + 0x78][10:11]
tf = @32[RSP_init + 0x78][8:9]
i_f = @32[RSP_init + 0x78][9:10]
iop1_f = @32[RSP_init + 0x78][12:14]
nt = @32[RSP_init + 0x78][14:15]
rf = @32[RSP_init + 0x78][16:17]
vm = @32[RSP_init + 0x78][17:18]
ac = @32[RSP_init + 0x78][18:19]
vif = @32[RSP_init + 0x78][19:20]
vip = @32[RSP_init + 0x78][20:21]
i_d = @32[RSP_init + 0x78][21:22]
exception_flags = @32[RSP_init + 0x78][8:9]?(0x2,exception_flags_init)
IRDst = @64[RBP_init + 0x74]
@32[RBP_init + 0xFF] = 0x0

```

*Figure 31. Virtual registers of the second machine being mapped back to the native ones at the end of the virtual instruction*

**Analysis of the virtual context.** In this section we analyze the behavior of the first VM based on the results of the *Error! Reference source not found.* section.

Figure 32 shows:

- virtual registers being pushed onto the stack at the beginning of the prologue (red)
- partially the way the next virtual instruction is prepared to be executed (green)
- the virtual program counter being increased (blue)

In particular, the virtual program counter is represented by `@64[@64[RBP_init + 0x38] + 0x2C]`, where the register at `@64[RBP_init + 0x38]` holds the address of the virtual context. We can see that size of the initial virtual instruction was 8 bytes, since the virtual program counter is increased by 8 in the line highlighted with blue in Figure 32.

```

    . . .
@64[RBP_init + 0x137] = @64[RBP_init + 0x38] + 0x26
@32[@64[RBP_init + 0x38] + 0x26] = @32[RBP_init + 0x30] | @32[@64[RBP_init + 0x38] + 0x26]
@64[RBP_init + 0x50] = (@64[RBP_init + 0x30] & 0xFFFF)?({0x2 0 2, parity(@64[RBP_init + 0x30])})
@64[RBP_init + 0x30] = @64[RBP_init + 0x30] & 0xFFFF
@64[RBP_init + 0x50] = (@64[RBP_init + 0x30] << 0x3)?(@64[RBP_init + 0x30][61:62] 0 1, 0x0 16)
@64[RBP_init + 0x30] = @64[RBP_init + 0x30] << 0x3
@64[RBP_init + 0xDE] = @64[RBP_init + 0x30] + @64[RBP_init + 0xDE]
@64[RBP_init + 0x50] = {(@64[RBP_init + 0x30] ^ @64[RBP_init + 0xDE] ^ ((@64[RBP_init + 0x30] << 0x3) & 0xFFFF))}
@64[RBP_init + 0x74] = @64[@64[RBP_init + 0xDE]]
@64[RBP_init + 0xF2] = @64[RBP_init + 0x38]
@64[RBP_init + 0xF2] = @64[RBP_init + 0x38] + 0x2C
@64[@64[RBP_init + 0x38] + 0x2C] = @64[@64[RBP_init + 0x38] + 0x2C] + 0x8
@64[RBP_init + 0x50] = {(@64[@64[RBP_init + 0x38] + 0x2C] ^ ((@64[@64[RBP_init + 0x38] + 0x2C] << 0x3) & 0xFFFF))}
@64[RSP_init + 0xFFFFFFFFFFFFFFF8] = @64[RBP_init + 0xE6]
@64[RBP_init + 0x141] = @64[RBP_init + 0x141] + 0xFFFFFFFFFFFFFFF8
@64[RSP_init + 0xFFFFFFFFFFFFFFF8] = @64[RBP_init + 0x50]
@64[RBP_init + 0x141] = @64[RBP_init + 0x141] + 0xFFFFFFFFFFFFFFF8
@64[RSP_init + 0xFFFFFFFFFFFFFFF8] = @64[RBP_init + 0xE6]
@64[RBP_init + 0x141] = @64[RBP_init + 0x141] + 0xFFFFFFFFFFFFFFF8
@64[RSP_init + 0xFFFFFFFFFFFFFFF8] = @64[RBP_init + 0x98]
@64[RBP_init + 0x141] = @64[RBP_init + 0x141] + 0xFFFFFFFFFFFFFFF8
@64[RSP_init + 0xFFFFFFFFFFFFFFF8] = @64[RBP_init + 0x10D]
@64[RBP_init + 0x141] = @64[RBP_init + 0x141] + 0xFFFFFFFFFFFFFFF8
    . . .

```

Figure 32. Last few virtual instructions executed before mapping the virtual registers back to the native ones

As one can see in Figure 31 ( $IRDst = @64[RBP\_init + 0x74]$ ), the virtual register at offset  $0x74$  determines  $IRDst$  – the address of the next instruction. If we follow the virtual register  $@64[RBP\_init + 0x74]$  in Figure 32, we can see that it appears to be preparing to execute the next virtual instruction similarly to the second VM. Its [code slice](#) is the following series of expressions:

```

@64[RBP_init + 0x30] = @64[@64[RBP_init + 0x38] + 0x2C]
@64[RBP_init + 0x30] = @64[RBP_init + 0x30] + 0x2
@64[RBP_init + 0x30] = {@16[@64[RBP_init + 0x30]] 0 16, 0x0 16
64}

```



```

@32[RBP_init + 0x30] = @32[RBP_init + 0x30] + 0x8E839329
@64[RBP_init + 0x30] = @64[RBP_init + 0x30] & 0xFFFF
@64[RBP_init + 0x30] = @64[RBP_init + 0x30] << 0x3
@64[RBP_init + 0xDE] = @64[@64[RBP_init + 0x38] + 0xEE]
@64[RBP_init + 0xDE] = @64[RBP_init + 0x30] + @64[RBP_init +
0xDE]
@64[RBP_init + 0x74] = @64[@64[RBP_init + 0xDE]]

```

The entire slice of `@64[RBP_init + 0x30]` is meant just to acquire the offset of the next virtual instruction (opcode): it gets the virtual instruction's offset from the bytecode whose pointer is stored in the `@64[@64[RBP_init + 0x38] + 0x2C]` register, and the offset is subsequently increased by `0x8E839329`... which could have been omitted and serves solely to obscure the virtual instruction.

The virtual register `@64[@64[RBP_init + 0x38] + 0xEE]` contains the address of the virtual instruction table. Now it is clear that the first VM is obfuscated using known values from the bytecode too and that the code indeed executes a next virtual instruction as well – it definitely uses Direct Threading.

One can additionally see that `@64[RBP_init + 0x50]` stores the RFLAGS in Figure 32.

**Behavior.** The virtual instruction behaves similarly to the virtual instructions from the second VM – offsets of the virtual registers to be used are fetched from the virtual instruction's operands.

Subsequently a virtual register's value is moved to a memory address stored in another one: `[<virt_reg_1>] = <virt_reg_2>`. The target register is then either increased or decreased by 8: `<virt_reg_1> = <virt_reg_1> +/- 8`. This is most likely a PUSH instruction prepared also for environments where the stack grows upwards.

## 4.3 Initially executed virtual instructions

We will have a look at a few other virtual instructions to confirm our findings and the correctness of methods for analysis of the first VM. Specifically, the virtual instructions that are initially executed as we can compare the first VM's initial behavior to the second VM's.

**The first executed virtual instruction.** We can see in the highlighted line of Figure 33 that the first executed instruction of the first VM behaves indeed just like the one in the second VM – it just zeroes out an internal register and prepares another virtual instruction to be executed.

```

      . . .
@64[RBP_init + 0x141] = RSP_init + 0x98

@64[RBP_init + 0x88] = @64[RBP_init + 0x38]

@64[RBP_init + 0x88] = @64[RBP_init + 0x38] + 0x47
@64[RBP_init + 0x50] = {(@64[RBP_init + 0x38] ^ ((@64[RBP_init + 0x38] ^ (
@32[@64[RBP_init + 0x38] + 0x47] = 0x0

@64[RBP_init + 0x98] = 0x0

@64[RBP_init + 0x30] = @64[RBP_init + 0x38]

@64[RBP_init + 0x50] = {(@64[RBP_init + 0x38] ^ ((@64[RBP_init + 0x38] ^ (
@64[RBP_init + 0x30] = @64[RBP_init + 0x38] + 0x2C

@64[RBP_init + 0x30] = @64[@64[RBP_init + 0x38] + 0x2C]

@64[RBP_init + 0x50] = {(@64[RBP_init + 0x30] ^ ((@64[RBP_init + 0x30] ^ (
@64[RBP_init + 0x30] = @64[RBP_init + 0x30] + 0x2

@16[RBP_init + 0x98] = @16[@64[RBP_init + 0x30]]

@64[RBP_init + 0x98] = @64[RBP_init + 0x98] << 0x3
@64[RBP_init + 0x50] = (@64[RBP_init + 0x98] << 0x3)?(@64[RBP_init + 0x98]

@64[RBP_init + 0x74] = @64[RBP_init + 0x38]

@64[RBP_init + 0x74] = @64[RBP_init + 0x38] + 0xEE
@64[RBP_init + 0x50] = {(@64[RBP_init + 0x38] ^ ((@64[RBP_init + 0x38] ^ (
@64[RBP_init + 0xF2] = @64[@64[RBP_init + 0x38] + 0xEE]

@64[RBP_init + 0xF2] = @64[RBP_init + 0x98] + @64[RBP_init + 0xF2]
@64[RBP_init + 0x50] = {(@64[RBP_init + 0x98] ^ @64[RBP_init + 0xF2] ^ ((@
@64[RBP_init + 0x12B] = @64[@64[RBP_init + 0xF2]]

@64[RBP_init + 0x30] = @64[RBP_init + 0x38]

@64[RBP_init + 0x50] = {(@64[RBP_init + 0x38] ^ ((@64[RBP_init + 0x38] ^ (
@64[RBP_init + 0x30] = @64[RBP_init + 0x38] + 0x2C

@64[@64[RBP_init + 0x38] + 0x2C] = @64[@64[RBP_init + 0x38] + 0x2C] + 0x4
      . . .

```

*Figure 33. Zeroing out an internal register*

Statistics in Table 3 have been extracted from the processing of the first executed virtual instruction.

*Table 3. Statistics of the first executed virtual instruction*

Size of the bytecode block in bytes	548
Total number of processed virtual instructions	62
Total number of underlying native instructions	9,444
Total number of resulting IR instructions (including <code>IRDsts</code> )	195
Execution time in seconds	6.4810

**The second executed virtual instruction.** The second virtual instruction just zeroes out several internal registers, which are most likely about to be used for obfuscation, as in the second VM.

Statistics in Table 4 have been extracted from the processing of the second executed virtual instruction.

*Table 4. Statistics of the second executed virtual instruction*

Size of the bytecode block in bytes	755
Total number of processed virtual instructions	83
Total number of underlying native instructions	13,740
Total number of resulting IR instructions (including <code>IRDsts</code> )	259
Execution time in seconds	7.7718

**The third executed virtual instruction.** The third virtual instruction behaves just like the third one of the second VM too – it stores the stack pointer (highlighted in Figure 34). The addition of `0x98` is present due to applied optimizations which took into account the previously executed `POP` instructions in the **Prologue** section.

```

      . . .
@64[RBP_init + 0xDE] = @64[@64[RBP_init + 0x38] + 0x2C]
@64[RBP_init + 0x50] = {0x2 0 2, parity(@64[RBP_init + 0xDE] & 0xFF) 2 3, 0}
@64[RBP_init + 0xAC] = {@16[@64[RBP_init + 0xDE]] 0 16, 0x0 16 64}
@64[RBP_init + 0xAC] = @64[RBP_init + 0x38] + @64[RBP_init + 0xAC]
@64[RBP_init + 0x50] = {(@64[RBP_init + 0x38] ^ @64[RBP_init + 0xAC] ^ (@64[RBP_init + 0x38] ^ @64[RBP_init + 0xAC]))
@64[@64[RBP_init + 0xAC]] = RSP_init + 0x98
@64[RBP_init + 0x10D] = @64[RBP_init + 0xDE]
@64[RBP_init + 0xDE] = @64[RBP_init + 0x10D]

@64[RBP_init + 0xAC] = 0x0

@64[RBP_init + 0xC1] = @64[RBP_init + 0x38]
@64[RBP_init + 0xC1] = @64[RBP_init + 0x38] + 0x2C
@64[RBP_init + 0x50] = {(@64[RBP_init + 0x38] ^ (@64[RBP_init + 0x38] ^ (@64[RBP_init + 0x38] ^ @64[RBP_init + 0x38])))
@64[RBP_init + 0xC1] = @64[@64[RBP_init + 0x38] + 0x2C]
@64[RBP_init + 0xC1] = @64[RBP_init + 0xC1] + 0x2
@64[RBP_init + 0x50] = {(@64[RBP_init + 0xC1] ^ (@64[RBP_init + 0xC1] ^ (@64[RBP_init + 0xC1] ^ @64[RBP_init + 0xC1])))
@16[RBP_init + 0xAC] = @16[@64[RBP_init + 0xC1]]
@64[RBP_init + 0xAC] = @64[RBP_init + 0xAC] << 0x3
@64[RBP_init + 0x50] = (@64[RBP_init + 0xAC] << 0x3)?{@64[RBP_init + 0xAC] << 0x3}
@64[RBP_init + 0x74] = @64[RBP_init + 0x38]
@64[RBP_init + 0x74] = @64[RBP_init + 0x38] + 0xEE
@64[RBP_init + 0x50] = {(@64[RBP_init + 0x38] ^ (@64[RBP_init + 0x38] ^ (@64[RBP_init + 0x38] ^ @64[RBP_init + 0x38])))
@64[RBP_init + 0x10D] = @64[@64[RBP_init + 0x38] + 0xEE]
@64[RBP_init + 0x10D] = @64[RBP_init + 0xAC] + @64[RBP_init + 0x10D]
@64[RBP_init + 0x50] = {(@64[RBP_init + 0xAC] ^ @64[RBP_init + 0x10D] ^ (@64[RBP_init + 0x38] ^ @64[RBP_init + 0x10D]))
@64[RBP_init + 0x58] = @64[@64[RBP_init + 0x10D]]
@64[RBP_init + 0x105] = @64[RBP_init + 0x38]
@64[RBP_init + 0x105] = @64[RBP_init + 0x38] + 0x2C
@64[@64[RBP_init + 0x38] + 0x2C] = @64[@64[RBP_init + 0x38] + 0x2C] + 0x4
      . . .

```

Figure 34. Storing the stack pointer in an internal register

Statistics in Table 5 have been extracted from the processing of the third executed virtual instruction.

*Table 5. Statistics of the third executed virtual instruction*

Size of the bytecode block in bytes	586
Total number of processed virtual instructions	66
Total number of underlying native instructions	10,263
Total number of resulting IR instructions (including IRDsts)	207
Execution time in seconds	6.8428

**The fourth executed virtual instruction.** We naturally expect this instruction to be a POP as in the second VM; however, it is hard to confirm statically as the already described obfuscation techniques make it too hard to understand. One can see part of the virtual instruction in Figure 35.

Statistics in Table 6 have been extracted from the processing of the fourth executed virtual instruction.

*Table 6. Statistics of the fourth executed virtual instruction*

Size of the bytecode block in bytes	4,883
Total number of processed virtual instructions	425
Total number of underlying native instructions	71,192
Total number of resulting IR instructions (including IRDsts)	1,038
Execution time in seconds	28.1638

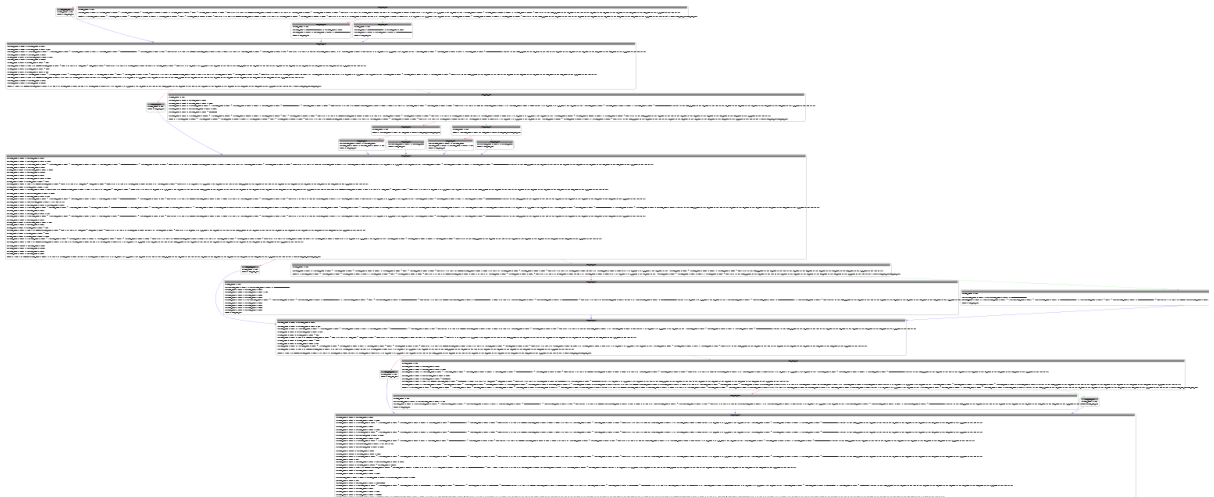


*Figure 35. Part of the fourth virtual instruction*

When we look closely at certain parts of Figure 35, it appears to be able to behave as a POP instruction. The part of the virtual instruction in Figure 36 clearly behaves just like the fourth one of the second VM – it moves a value off the top of the stack, and if the target register is different from the stack pointer, the stack pointer is increased.

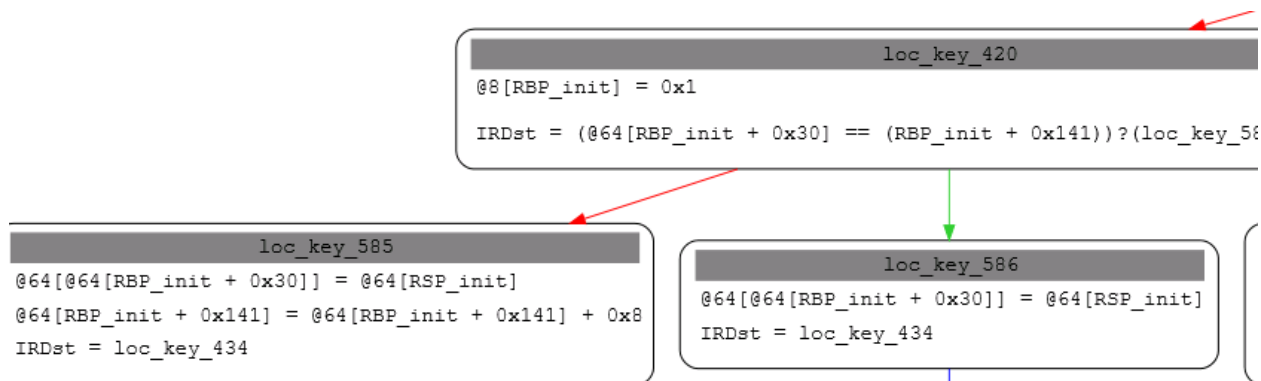


Figure 36. Part of the fourth virtual instruction performing a pop-like operation

**Instruction merging.** However, the instruction also seems to be capable of performing a PUSH and other operations as well, based on the operands (Figure 37), which means that it consists of several other instructions merged into one, which is a kind of [obfuscation technique](#). It most likely merged several instructions with different rolling keys into one.

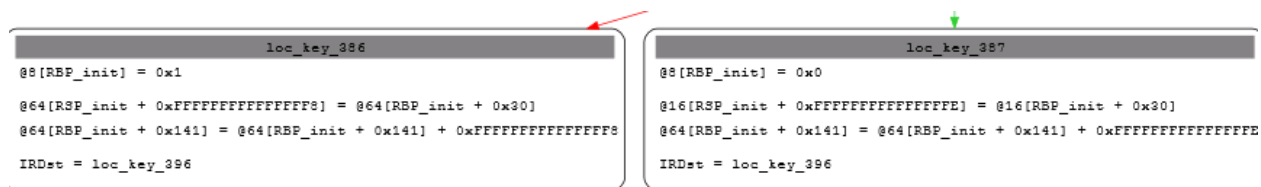


Figure 37. Part of the fourth virtual instruction performing a PUSH operation

## 5 Automating analysis of the first virtual machine

Now that we know what the internal structure of the first VM is like, we can process the VM as the second one since analyzing all the virtual instructions would be complicated due to the additional obfuscation techniques – we can again effectively eliminate them with symbolic execution.

We definitely need to concretize the virtual instruction table and internal registers dedicated for obfuscation as in the previous one, which is not complicated. The question is: What do we do with the second VM?

There is a pretty simple solution – instead of preserving the entire context of the second VM and working with both at once, we can simply concretize the entire second VM as we know what memory ranges belong to the VMs.

We will also ignore all memory assignments to the second VM’s context and not preserve any information about its structure. This will enable us to focus only on the first one and build the same graph as before.

We could also preserve the obfuscated IR of all the virtual instructions of the first VM and use them instead – it would save a significant amount of time during the processing since we would not repeatedly disassemble, translate and deobfuscate the second VM for each opcode in the bytecode blocks of the first VM. However, we want to show that it is possible to process both layers at once.

**Processing the initial bytecode block.** We processed the very first bytecode block as was described in the previous section. The resulting code still appears to be too complex since we expected a series of POPs, the deobfuscated code and then a series of PUSHes and finally mapping back to the native registers. However, there are additional, multiple branches. One can see part of the code in Figure 38.



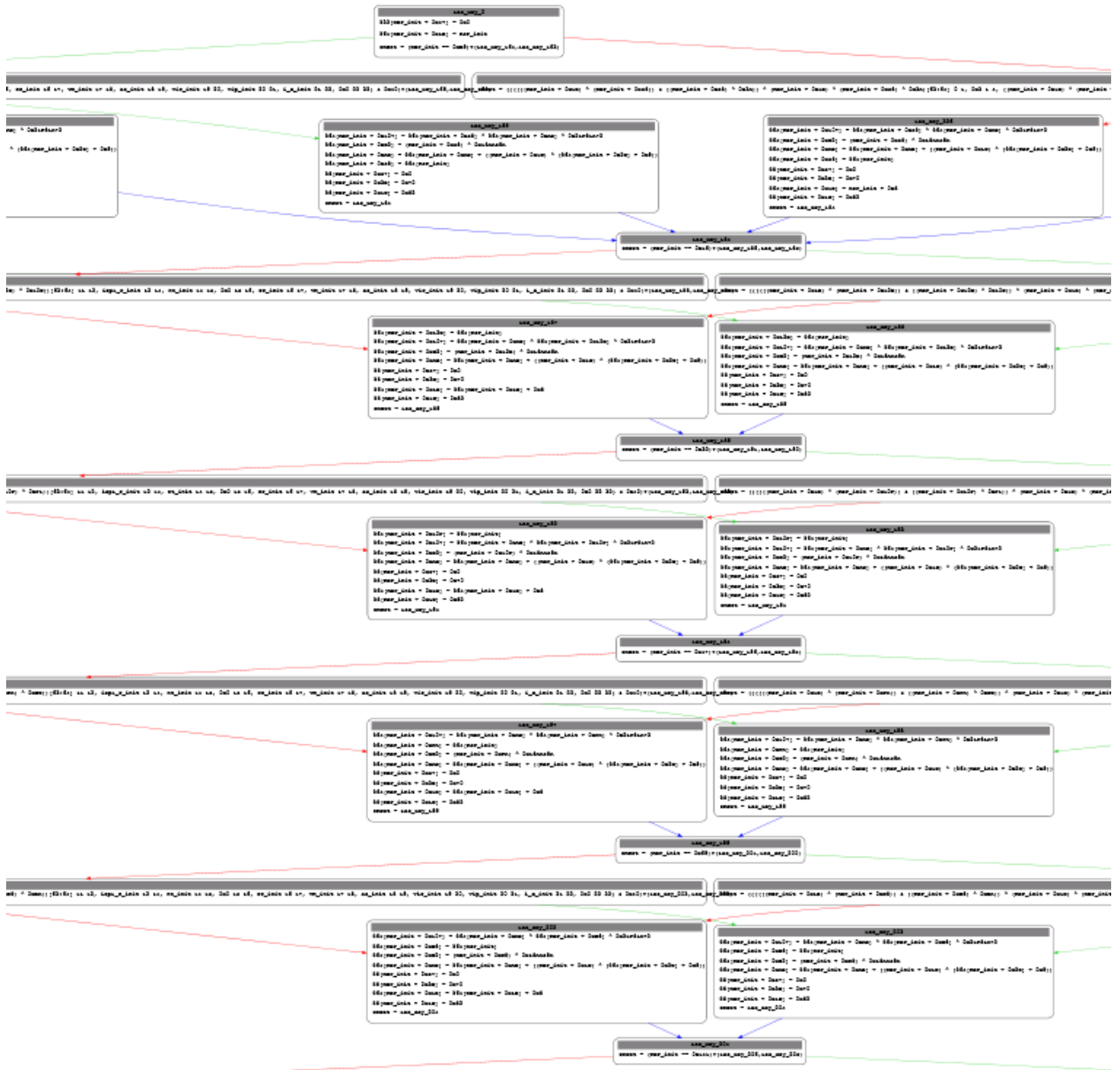


Figure 38. The first processed bytecode block

**Opaque predicates.** Looking at the code more closely, we notice two types of expressions that can be further simplified. The first is the value of `RBP_init`, which is the address of the virtual context and it is known (Figure 39).

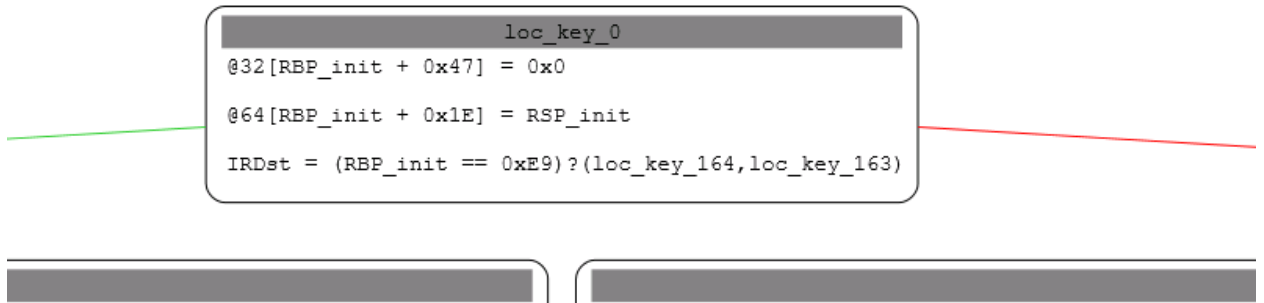


Figure 39. Expressions that can be further simplified

Both paths that follow the initial block in Figure 39 contain the same code, hence this is not the same case as with the POP virtual instruction, where it was important to know what the target register was because it determined the subsequent behavior of the virtual instruction. These checks are, on the other hand, unimportant and we can just get rid of them – they can be considered as a sort of opaque predicate [19].

Note that the branch of the POP virtual instruction was now optimized out automatically since offsets of the registers were present in the bytecode and directly known.

Finally, these were the last obfuscation techniques, and we can look at the simplified code.

**Overview.** We are finally greeted with a familiar, even pleasant, view in Figure 40 – as expected the code begins with a series of POPs (red) and ends with a series of PUSHes (green) that represent parts of the context switches.

Another interesting detail is that the VM uses a special internal register to store the destination address – the final jump is not visible, but the code jumps to `@64[RBP_init + 0x133]`. As was mentioned earlier, the VM also stores the base address of its code section; this is stored in virtual register `@64[RBP_init + 0x80]` in our case.

One can see that the code in Figure 40 also accesses certain data using the base address, specifically at offset `0x0E3808` (blue). After looking up the address, we found that it belongs to a `ServiceStatus` structure (Figure 41).

```

@64[RBP_init + 0x1E] = RSP_init + 0x70
@64[RBP_init + 0x15] = @64[RSP_init]
@64[RBP_init + 0x11F] = @64[RSP_init]
@64[RBP_init + 0x1E] = RSP_init + 0x78
@64[RBP_init + 0x4F] = @64[RSP_init]
@64[RBP_init + 0x1E] = RSP_init + 0x80
@64[RBP_init + 0xCC] = @64[RSP_init]
@64[RBP_init + 0x1E] = RSP_init + 0x88

@64[RBP_init + 0x1E] = RSP_init + 0x98
@64[RBP_init + 0x13F] = @64[@64[RBP_init + 0x13F]]
@32[RBP_init + 0x53] = 0x0
@32[RBP_init + 0x4F] = 0x1C

@64[RBP_init + 0x133] = 0x3092
@64[RBP_init + 0x133] = @64[RBP_init + 0x80] + 0x3092
@64[RBP_init + 0x133] = @64[RBP_init + 0x80] + 0xE3808
@64[RBP_init + 0x74] = @64[RBP_init + 0x80] - 0xE3808
IRDst = loc_key_291

```

---

```

loc_key_291
x1 6 7, (@64[RBP_init + 0x4F] + 0xFFFFFFFFFFFFFFFF)[63:64] 7 8, @32[RBP_init + 0xCC][8:11] 8 11, ((@64[RBP_init + 0x4F] ^ (@64[RBP_init + 0x4F] + 0xFFFFFFFF

```

---

```

20, vip_init 20 21, i_d_init 21 22, 0x0 22 32) & 0x40, {0x2 0 2, parity(@32[RBP_init + 0xCC] & 0x40) 2 3, 0x8 3 8, tf_init 8 9, i_f_init 9 10, df_init 10 11,

```

---

```

loc_key_318
@64[RBP_init + 0x133] = 0x30A2
@64[RBP_init + 0x133] = @64[RBP_init + 0x80] + 0x30A2
@64[RBP_init + 0x133] = @64[RBP_init + 0x80] + 0x2FB0
@64[RBP_init + 0x15] = @64[RBP_init + 0x80] + 0x2FB0
@64[RBP_init + 0x11F] = @64[RBP_init + 0x13F]
@64[RBP_init + 0x133] = 0x30AB
@64[RBP_init + 0x133] = @64[RBP_init + 0x80] + 0x30AB
@64[RBP_init + 0x133] = @64[RBP_init + 0x80] + 0x3C098
@64[RBP_init + 0xFFFFFFFFFFFFFFFF3] = @64[RBP_init + 0x4F]
@64[RBP_init + 0x1E] = @64[RBP_init + 0x1E] + 0xFFFFFFFFFFFFFFFF

```

Figure 40. Code of the processed bytecode

```

.data:000007FEB5FF3808 ; struct _SERVICE_STATUS ServiceStatus
.data:000007FEB5FF3808 ServiceStatus _SERVICE_STATUS <0>
.data:000007FEB5FF3808

```

Figure 41. Data accessed by the code – ServiceStatus

It additionally sets a register before recovering the native state to a data address at offset 0x2FB0 (yellow). The address contains a non-obfuscated function shown in Figure 42.

```

.text:000007FEB5F12FB0
.text:000007FEB5F12FB0
.text:000007FEB5F12FB0 sub_7FEB5F12FB0 proc near
.text:000007FEB5F12FB0 var_8= qword ptr -8
.text:000007FEB5F12FB0 000 sub    rsp, 28h
.text:000007FEB5F12FB4 028 cmp     ecx, 1
.text:000007FEB5F12FB7 028 jnz    loc_7FEB5F13065

.text:000007FEB5F12FBD 028 mov     rcx, cs:hServiceStatus ; hServiceStatus
.text:000007FEB5F12FC4 028 inc     cs:ServiceStatus.dwCheckPoint

.text:000007FEB5F12FCA
.text:000007FEB5F12FCA loc_7FEB5F12FCA:
.text:000007FEB5F12FCA 028 mov     [rsp+28h+var_8], rbx
.text:000007FEB5F12FCF 028 lea    rdx, ServiceStatus ; lpServiceStatus
.text:000007FEB5F12FD6 028 xor     ebx, ebx
.text:000007FEB5F12FD8 028 mov     cs:ServiceStatus.dwCurrentState, 3
.text:000007FEB5F12FE2 028 mov     qword ptr cs:ServiceStatus.dwControlsAccepted, 1
.text:000007FEB5F12FED 028 mov     cs:ServiceStatus.dwWaitHint, ebx
.text:000007FEB5F12FF3 028 call   cs:SetServiceStatus
.text:000007FEB5F12FE9 028 cmp     cs:dword_7FEB5F3790, ?

```

Figure 42. Function whose pointer is used in the code

Let us now focus on the destination address (gray) – it is set to <base address> + 0x8C038. Looking up that address in the sample, we see it belongs to the Windows API RegisterServiceCtrlHandlerW, which makes sense as the application is a service (Figure 43).

```

.idata:000007FEB5F9C038 ; SERVICE_STATUS_HANDLE __stdcall RegisterServiceCtrlH
.idata:000007FEB5F9C038 RegisterServiceCtrlHandlerW dq offset advapi32_Registe
.idata:000007FEB5F9C040 db 0, 0, 0, 0, 0, 0, 0, 0

```

Figure 43. Destination address of the bytecode

The question is now, what is the return address of the API call. When we look at the end of the code, we see that it sets the return address – the highlighted assignment in Figure 44 appears to be 0x88 bytes above the stack pointer, but we need to keep in mind that we started below the stack pointer because we did not perform the initial context pushing from `vm_init()` and in reality, it is the return address.

The return address is set to another `vm_pre_init()`.

```

@64[RSP_init + 0x88] = @64[RBP_init + 0x80] + 0x21EA5C
@32[RBP_init + 0x127] = 0x0
RAX.0 = @64[RSP_init + 0x70]
RSP.0 = RSP_init + 0x88
exception_flags = @32[RSP_init + 0x78][8:9]? (0x2, exception_flags_init)
IRDst = @64[@64[RBP_init + 0x133]]

```

Figure 44. Setting return address of the API call

The last part of the code that needs to be analyzed is the body of the loop (Figure 45). It is pretty simple – it zeroes out a memory range. If we look back at Figure 40 and look up what is in `@64[RBP_init + 0x74]`, we see that it is set to the address of the `ServiceStatus` structure (blue) – this piece of code zeroes out the structure. Meanwhile, `@64[RBP_init + 0x4F]` (pink in Figure 40) initially contains the constant `0x1C` – size of the structure – and `@64[RBP_init + 0xCC]`, the CPU flags.

```

@64[RBP_init + 0xCC] = {@32[RBP_init + 0xCC][0:1] 0 1, 0x1 1 2, parity
@64[RBP_init + 0x4F] = @64[RBP_init + 0x4F] + 0xFFFFFFFFFFFFFFFF
@64[RBP_init + 0x133] = @64[RBP_init + 0x4F]
@64[RBP_init + 0x133] = @64[RBP_init + 0x4F] + @64[RBP_init + 0x74]
@8[@64[RBP_init + 0x4F] + @64[RBP_init + 0x74]] = 0x0
IRDst = ((@32[RBP_init + 0xCC] & 0x40)?({0x2 0 2, parity(@32[RBP_init

```

Figure 45. Body of the code's loop

Now we look at the discovered non-obfuscated sample and compare it against our findings. We can confirm that we deobfuscated the first bytecode block successfully (Figure 46).

```

public ServiceMain
ServiceMain proc near

arg_0= qword ptr 8
arg_8= qword ptr 10h

} 48 89 5C 24 10      mov     [rsp+10h], rbx
} 57                  push   rdi
} 48 83 EC 20         sub    rsp, 20h
} 48 8B 1A           mov    rbx, [rdx]
} B8 1C 00 00 00     mov    eax, 28
} 48 8D 3D AF 07 0E 00 lea   rdi, ServiceStatus
} 0F 1F 80 00 00 00 00 nop    dword ptr [rax+00000000h]

loc_180003060:
}28 48 FF C8         dec    rax
}28 C6 04 38 00     mov    byte ptr [rax+rdi], 0
}28 75 F7           jnz   short loc_180003060

8D 15 10 FF FF FF   lea   rdx, HandlerProc ; lpHandlerProc
8B CB               mov   rcx, rbx ; lpServiceName
15 BF 8F 08 00     call  cs:RegisterServiceCtrlHandlerW
89 05 B0 07 0E 00   mov   cs:hServiceStatus, rax
85 C0               test  rax, rax
78                  jz    short loc_1800030FD

```

Figure 46. The same part of code in the non-obfuscated binary

Statistics in Table 7 have been extracted from the processing of the first bytecode block.

Table 7. Statistics of the first processed bytecode block

Size of the bytecode block in bytes	695
Total number of processed virtual instructions	62
Total number of underlying native instructions	3,536,427
Total number of resulting IR instructions (including IRDsts)	192
Execution time in seconds	382.5678

## 6 Description of our final VM analyzer code

Our final analyzer code consists of several classes that interact together, as described in the following sections. The full code listing is available in our GitHub repository `github.com/eset/wslink-vm-analyzer`. The classes follow the high-level descriptions from the previous Automating analysis sections.

**Class `Wslink`.** `Wslink` is a mediator that handles interaction of the remaining classes, its constructor processes the supplied memory dump, and its method `process()` accepts the value of the virtual program counter – pointer to the bytecode – with the opcode of the initial instruction. The bytecode is subsequently processed using classes `VirtualContext`, `SymbolicCFG` and `MySymbolicExecutionEngine`; the resulting control flow graph is written into a DOT [17] file `vma.dot`.

Parts of the VM, such as address of the instruction table or offsets of the virtual registers for obfuscation, should be overwritten to provide specific values for individual VMs.

**Class `VirtualContext`.** This class represents the virtual context – it contains most notably the initial values of the virtual registers for obfuscation, virtual program counter, and the address of the instruction table.

It also provides several methods for working with the context described in the following sections.

**Method `VirtualContext::get_next_instr()`.** The method `get_next_instr()` applies the address of the instruction table to the destination address to simplify the corresponding expression and attempts to unambiguously determine the address of the next virtual instruction to be executed.

**Method `VirtualContext::get_irb_syms()`.** This method simply acquires the expressions that should be preserved in the nodes of the resulting control flow graph.

**Method `VirtualContext::get_updated_internal_context()`.** The method `get_updated_internal_context()` updates values of the internal registers that need to be preserved between virtual instructions, such as the virtual program counter or the obfuscation registers.

**Method `VirtualContext::get_state_hash()`.** This method calculates a hash for virtual instructions – the hash is used to specify the actual position in the bytecode to reconstruct the control flow graph without duplicate nodes or paths and to avoid infinite loops in cycles. It is calculated just from the virtual program counter.

**Class `MySymbolicExecutionEngine`.** This class overrides the method `mem_read()` of Miasm’s class `SymbolicExecutionEngine` primarily to transform memory accesses relative to the virtual program counter and the virtual instruction table into concrete values. It is additionally meant to make the second VM completely concrete when we are processing the first one.

**Class `SymbolicCFG`.** This class is meant to construct the resulting control flow graph. It uses class `Node` to process individual virtual instructions, to acquire the expressions that need to be preserved, and to determine addresses of the next virtual instructions.

Each `Node` is tied to a hash generated by `get_state_hash()` (as described above) and the address, `StateID`, of the block of code that is being processed. This means that virtual instructions containing unbounded loops cannot currently be processed correctly because when we connect a state to an already processed one, it will not take into account the changes introduced in the body of the loop.

**Class `Node`.** This class simply represents a node in the resulting control flow graph – it most notably contains the values of the obfuscation registers and virtual program counter that are together called `init_symbols`. These are the values required to determine the addresses of the next virtual instructions.



It provides a method `process_addr()` that can get the following `Nodes` classes that have not yet been processed and return them along with the expressions that should be preserved in a data-class `ContextResult`.

The new `Nodes` are created based on the supplied addresses using method `_get_next()`, which accepts several arguments. The arguments can instruct the function to slightly modify the resulting `Node` – make a copy of the actual symbolic state when there is a branch, or update `init_symbols` for a new virtual instruction.

## 7 Future work

Once we discovered a non-obfuscated sample, we were not motivated to completely deobfuscate the rest of the code.

Our next steps would consist of:

1. Getting rid of the prologue and epilogue and mapping the virtual registers directly to the native ones.
2. Automatically processing the subsequent bytecode blocks and extending the graph with resulting code listings to get an overview of the whole function.
3. Optionally addressing individual instructions with unbounded loops that cannot be fully processed using symbolic execution (e.g., instructions like `DEC_RC4` mentioned in Miasm's blog [9]) and manually creating their IR to be added to the graph. We could also experiment with some enhancements of symbolic execution that attempt to mitigate the issue [18].
4. Optionally matching resulting IR expressions against known IR expressions of assembly instructions to recover assembly code.

# Conclusion

We have described internals of an advanced multilayered virtual machine of CodeVirtualizer and successfully designed and implemented a semiautomatic solution capable of significantly facilitating analysis of the program's code. This virtual machine introduced several other obfuscation techniques such as junk code, encoding of virtual operands, duplication of virtual opcodes, opaque predicates, merging of virtual instructions and a nested virtual machine to further obstruct reverse engineering of the code that it protects, yet we successfully overcame them all.

To deal with the obfuscation we modified a known technique that extracts the semantics of the virtual opcodes using symbolic execution with simplifying rules. Additionally, we made concrete the internal virtual registers for obfuscation along with memory accesses relative to the virtual program counter to automatically apply known values and deobfuscate semantics of the virtual instructions – this additionally broke down boundaries between individual virtual instructions. Boundaries are necessary to prevent path explosion of the symbolic execution; we would lose track of the virtual program counter – our position in the interpreted code – without them. We defined new boundaries by symbolizing the address of the virtual instruction table, since it is required to get the next instruction, and concretized it only when we needed to move to the following virtual instructions. We subsequently constructed a control flow graph of the original code in an intermediate representation from one of the bytecode blocks based on the virtual program counter, and extracted deobfuscated semantics of individual virtual instructions. We finally extended the approach to process both virtual machines at once by entirely concretizing the nested one.

# References

- [1] Vladislav Hrčka, Under the hood of Wslink’s multilayered virtual machine, cited on:10.4.2022, available online:<https://www.welivesecurity.com/2022/03/28/under-hood-wslink-multilayered-virtual-machine/>
- [2] David A. Patterson and John L. Hennessy, Computer Organization and Design – The Hardware / Software Interface, 4th.Edition, Morgan Kaufmann, Elsevier, 2009
- [3] Shi Y, Casey K, Ertl MA, Gregg D., Virtual machine showdown: Stack versus registers, ACM Transactions on Architecture and Code Optimization (TACO), 2008
- [4] Berndl M, Vitale B, Zaleski M, Brown AD, Context threading: A flexible and efficient dispatch technique for virtual machine interpreters, International Symposium on Code Generation and Optimization, 2005
- [5] Process Context, cited on:10.4.2022, available online:[tldp.org/LDP/LG/issue23/flower/context.html](http://tldp.org/LDP/LG/issue23/flower/context.html), The Linux Documentation Project
- [6] Moura LD, Bjørner N, Z3: An efficient SMT solver, International conference on Tools and Algorithms for the Construction and Analysis of Systems, pages 337-340, 2008
- [7] Sumit Gulwani, Program Synthesis, cited on:10.4.2022, available online:[microsoft.com/en-us/research/project/program-synthesis/](https://microsoft.com/en-us/research/project/program-synthesis/), Microsoft, 2010
- [8] Rolles R. Unpacking virtualization obfuscators, 3rd USENIX Workshop on Offensive Technologies, 2009
- [9] ZeusVM analysis, cited on:10.4.2022, available online:[mi-asm.re/blog/2016/09/03/zeusvm\\_analysis.html](http://mi-asm.re/blog/2016/09/03/zeusvm_analysis.html), 2016
- [10] Salwan J, Bardin S, Potet ML, Symbolic deobfuscation: From virtualized code back to the original, International Conference on Detection of Intrusions and Malware, and Vulnerability Assessment, pages 372-392, 2018
- [11] Blazytko T, Contag M, Aschermann C, Holz T, Syntia: Synthesizing the semantics of obfuscated code, 26th USENIX Security Symposium, pages 643-659, 2017
- [12] Desclaux F, Miasm: Framework de reverse engineering, SSTIC, 2012
- [13] Miasm, cited on:10.4.2022, available online:[github.com/cea-sec/miasm/tree/9a36c6d7849335c83a9460fc558afb55ff0a2aa1](https://github.com/cea-sec/miasm/tree/9a36c6d7849335c83a9460fc558afb55ff0a2aa1)

- [14] Vladislav Hřčka, Wslink: Unique and undocumented malicious loader that runs as a server, cited on:10.4.2022, available online:[welivesecurity.com/2021/10/27/wslink-unique-undocumented-malicious-loader-runs-server/](https://welivesecurity.com/2021/10/27/wslink-unique-undocumented-malicious-loader-runs-server/)
- [15] CodeVirtualizer, cited on:10.4.2022, available online:[oreans.com/CodeVirtualizer.php](https://oreans.com/CodeVirtualizer.php)
- [16] Anand S, Godefroid P, Tillmann N, Demand-driven compositional symbolic execution, International Conference on Tools and Algorithms for the Construction and Analysis of Systems, pages 367-381, 2008
- [17] DOT Language, cited on:10.4.2022, available online:[graphviz.org/doc/info/lang.html](https://graphviz.org/doc/info/lang.html)
- [18] Trtík M, Symbolic execution and program loops, Masaryk University Brno, 2013
- [19] Ming J, Xu D, Wang L, Wu D. Loop: Logic-oriented opaque predicate detection in obfuscated binary code, Proceedings of the 22nd ACM SIGSAC Conference on Computer and Communications Security, pages 757-768, 2015.